

BEST AVAILABLE COPY

2- (TULSA)
AN - 527840
TI - EXPERIMENTAL STUDY OF AN ADVANCED THREE-COMPONENT BOREHOLE SEISMIC RECEIVER
AU - SLEEFE, G E; ENGLER, B P
OS - SANDIA NATIONAL LABS
SO - SANDIA NAT LAB REP NO SAND-91-1265C (DE91014652) (1991) (1 MICROFICHE WITH 5 PP; 5 REFS)
LA - ENGLISH
DT - (GR) GOVERNMENT REPORT
IT - *THREE COMPONENT GEOPHONE; *CROSSHOLE METHOD; *EXPLORATION; *GEOPHONE; *GEOPHYSICAL EQUIPMENT; *GEOPHYSICAL EXPLORATION; *PROCEDURE;
*PROFILING;
*RECORDING; *SEISMIC EQUIPMENT; *SEISMIC EXPLORATION; *SEISMIC RECORDING;
*SEISMIC REFLECTION METHOD; *THREE COMPONENT RECORDING; *VERTICAL SEISMIC
PROFILING; ACCELEROMETER; BOREHOLE; CASINGS; CHART; CONNECTOR; COUPLING (MECHANICAL); DATA; DATA ACQUISITION; DEEP HOLE GEOPHONE; FINITE ELEMENT;
FITTING; FREQUENCY; GEOPHYSICAL DATA; GRAPH; HARRIS CO, TEX; HUMBLE OIL FIELD; INSTRUMENT; MATHEMATICS; NOISE; NORTH AMERICA; PHOTOGRAPH; PIEZOELECTRIC GEOPHONE; PRESSURE; REFLECTION (SEISMIC); SEISMIC DATA; SEISMIC NOISE; SEISMIC WAVE PROPAGATION; SIGNAL TO NOISE RATIO; SONDE; SUBSURFACE PRESSURE; SUBSURFACE TEMPERATURE; TEMPERATURE; TEXAS; TRANSMISSION (SEISMIC); UNITED STATES; WAVE FREQUENCY; WAVE PHENOMENON; WAVE PROPAGATION; WESTERN US
MH - *THREE COMPONENT GEOPHONE
CC - GEOPHYSICS
AB - AN ADVANCED 3-COMPONENT BOREHOLE SEISMIC RECEIVER HAS BEEN DESIGNED, DEVELOPED AND TESTED. THIS RECEIVER WAS DESIGNED WITH THE AID OF FINITE ELEMENT VIBRATION MODELING TO BE FREE OF SIGNIFICANT CLAMP RESONANCES BELOW 2,000 HZ. THIS BROAD FREQUENCY RANGE MAKES THIS SONDE WELL SUITED FOR CROSS-WELL SEISMIC IMAGING APPLICATIONS. STATE-OF-THE-ART PIEZOELECTRIC ACCELEROMETERS ARE USED AS THE 3-COMPONENT SENSORS AND PROVIDE SIGNAL ENHANCEMENT RELATIVE TO CONVENTIONAL GEOPHONES. THE USE OF THESE ACCELEROMETERS OFFER A SIGNAL-TO-NOISE ENHANCEMENT OF APPROX. 20 DB AT 1,000 HZ OVER MOVING-COIL SEISMIC GEOPHONES. A PROTOTYPE ACCELEROMETER-BASED SONDE WAS FIELD TESTED AT THE TEXACO HUMBLE FIELD TO DETERMINE ITS PERFORMANCE CHARACTERISTICS. THE ADVANCED SONDE EXHIBITED SIGNIFICANTLY IMPROVED COUPLING RELATIVE TO THE VSP (VERTICAL SEISMIC PROFILE) TOOL AS EVIDENCED BY INCREASED BANDWIDTH AND SIGNAL-TO- NOISE RATIO. ADDITIONALLY, THE ADVANCED SONDE PRODUCED SIGNALS WHICH RIVAL THOSE PRODUCED BY THE BURIED/CEMENTED GEOPHONES.

Logging in to Orbit

Trying 9228502...Open

ENTER ORBIT USERID

pt210jz7

WELCOME TO ORBIT ONLINE SERVICE. (10/09/98 12:12 P.M. CENTRAL TIME)

ENTER SECURITY CODE:

CLAIMS RELOAD 1998 FEATURING ANTICIPATED EXPIRATION DATES - NEWSDOC N296

NON-SUBSCRIBER ACCESS TO THE DERWENT WPI/API MERGED FILE - NEWSDOC N295

QUESTEL-ORBIT'S INTELLECTUAL PROPERTY GOLD PROJECT - NEWSDOC N294

DERWENT WPI NOW ADDS COVERAGE OF MEXICO - NEWSDOC N293

DERWENT WORLD PATENTS INDEX (WPAT) RELOADED - NEWSDOC N286
(OR TYPE: EXPLAIN WPAT)

QUESTEL-ORBIT MINIMUM BILLING POLICY - NEWSDOC N281

TO SEE AN INDEX OF ORBIT SYSTEM AND DATABASE NEWS - TYPE: NEWS
TO SEE THE TEXT OF A NEWSDOC - TYPE: NEWSDOC N###
TO DISPLAY A LIST OF 1998 DATABASE PRICES - TYPE: EXPLAIN PRICES

YOU ARE NOW CONNECTED TO ORBIT.

FOR A TUTORIAL, ENTER ? OTHERWISE, ENTER A COMMAND OR SS.

file tulsa

ELAPSED TIME ON ORBIT: 0.01 HRS.

\$0.46 EST COST CONNECT TIME.

\$0.46 EST TOTAL COST THIS ORBIT SESSION.

YOU ARE NOW CONNECTED TO TULSA.

COPYRIGHT 1965 TO PRESENT BY UNIVERSITY OF TULSA
COVERS 1965 THRU WK41 (9841)

SS 1?

gaiser, e j/au

TERM (GAISER, E J/AU) NOT FOUND.

SS 1 RESULT (0)

SS 2?

gaiser

TERM (GAISER) NOT FOUND.

SS 2 RESULT (0)

SS 3?
vertical (s) seismic (s) profile

*SEARCHING
OCCURS TERM
26772 VERTICAL
65881 SEISMIC
24557 PROFILE
SS 3 RESULT (625)

SS 4?
ss 3 and sonde

OCCURS TERM
3880 SONDE
SS 4 RESULT (15)

SS 5?
ss 4 and coupling

OCCURS TERM
14432 COUPLING
SS 5 RESULT (5)

SS 6?
d 1-5

TERM (D 1-5) NOT FOUND.
SS 6 RESULT (0)

SS 7?
print scanplus 1-5

RECORDS SELECTED FROM SS 5.

-1- (TULSA)
AN - 652963
TI - PERMANENT, DOWNHOLE SEISMIC SENSORS FOR RESERVOIR MONITORING
AU - BATHELLIER, E J M; CZERNICHOW, J A
PY - 97

-2- (TULSA)
AN - 527840
TI - EXPERIMENTAL STUDY OF AN ADVANCED THREE-COMPONENT BOREHOLE SEISMIC
RECEIVER
AU - SLEEFE, G E; ENGLER, B P
PY - 91

-3- (TULSA)
AN - 464891
TI - LOCKING ARM FOR WELL TOOL
AU - PETERMANN, S G
PY - 89

-4- (TULSA)
AN - 435133
TI - VERTICAL SEISMIC PROFILE SONDE COUPLING
AU - GAISER, J E; FULP, T J; PETERMANN, S G; KARNER, G M
PY - 88

-5- (TULSA)
AN - 393612
TI - A LARGE (5') DIAMETER BOREHOLE SEISMIC LOGGING TOOL - VERTICAL SEISMIC
PROFILE AND OBLIQUE SEISMIC PROFILE APPLICATIONS (SONDE SISMIQUE POUR
FORAGE GRAND DIAMETRE - RESULTATS EN PROFIL SISMIQUE OBLIQUE
MULTI-OFFSET)
AU - RUZIE, G; BATOT, J; MARCHAND, J L
PY - 84

SS 7?
print full 2

RECORDS SELECTED FROM SS 5.

-1- (TULSA)
AN - 652963
TI - PERMANENT, DOWNHOLE SEISMIC SENSORS FOR RESERVOIR MONITORING
AU - BATHELLIER, E J M; CZERNICHOW, J A
OS - CREATECH INDUSTRIE
SO - J PETROL TECHNOL V 49, NO 5, PP 494,496, MAY 1997 (OTC-8309)
NU - ISSN 01492136
LA - ENGLISH
IT - *ENGINEERING GEOPHYSICS; *DOWNHOLE SEISMIC SOURCE; *ELASTIC WAVE;
*GEOPHONE; *GEOPHYSICAL EQUIPMENT; *GEOPHYSICS; *MICROSEISM;
*MONITORING;
*PERFORMANCE; *RESERVOIR PERFORMANCE; *SEISMIC EQUIPMENT; *SEISMIC WAVE;
*SEISMIC WAVE SOURCE; *TESTING; *THREE COMPONENT GEOPHONE; *WAVE; *WAVE
SOURCE; BOREHOLE; CABLE; CASED HOLE; CHART; COMPRESSIONAL WAVE;

CROSSHOLE
METHOD; ELECTRIC CABLE; ELECTRICAL EQUIPMENT; ELECTRONIC EQUIPMENT;
EXPLORATION; FRACTURING; FREQUENCY RESPONSE; GAS STORAGE WELL;
GEOPHYSICAL EXPLORATION; GRAPH; HODOGRAPH; HYDRAULIC FRACTURING;
INSTRUMENT; MOTION; PARTICLE MOTION; PROCEDURE; PROFILING; RECORD;
RECORDING; RESPONSE; SEISMIC EXPLORATION; SEISMIC RECORD; SEISMIC
REFLECTION METHOD; SHEAR WAVE; SONDE; THREE COMPONENT RECORDING; TUBING
CONVEYED OPERATION; VERTICAL SEISMIC PROFILING; WELL; WELL LOGGING
EQUIPMENT; WIRE LINE TOOL

MH - *ENGINEERING GEOPHYSICS
CC - WELL LOGGING & SURVEYING
AB - New seismic applications, such as microseismic monitoring, time-lapse
vertical seismic profile (VSP), and cross-well methods, have the
capability of resolving oil/gas structure details to dimensions of
approx. 3 ft, corresponding to an upper frequency limit of approx. one
kilohertz. Receivers must have a wideband frequency response, the
highest signal/noise ratio, and a response that is not modified by
artifacts related to the sondes design and must provide more complete
information by acquisition of both compressional- and shear-wave data.
Triaxial geophone sondes were developed that are capable of measuring
artifact-free frequency response over the 100- to 1,000-Hz frequency
range. The physical coupling of the sensors to the formation and the
accuracy of the geophones in responding to 3-component ground-particle
motion was critical to this application. The down-hole triaxial-
geophone sondes were designed for permanent and wireline installations,
and a sonde model is available for each phase of the well-completion

process. Designs include an outside-casing and an inside-casing sonde, an on-tubing or a through-tubing sonde. Example applications are discussed for hydraulic fracturing monitoring and gas storage well monitoring using both time-lapse VSP and microseismic data.

PY - 97

-2- (TULSA)
 AN - 527840
 TI - EXPERIMENTAL STUDY OF AN ADVANCED THREE-COMPONENT BOREHOLE SEISMIC RECEIVER
 AU - SLEEFE, G E; ENGLER, B P
 OS - SANDIA NATIONAL LABS
 SO - SANDIA NAT LAB REP NO SAND-91-1265C (DE91014652) (1991) (1 MICROFICHE WITH 5 PP; 5 REFS)
 LA - ENGLISH
 DT - (GR) GOVERNMENT REPORT
 IT - *THREE COMPONENT GEOPHONE; *CROSSHOLE METHOD; *EXPLORATION; *GEOPHONE; *GEOPHYSICAL EQUIPMENT; *GEOPHYSICAL EXPLORATION; *PROCEDURE; *PROFILING; *RECORDING; *SEISMIC EQUIPMENT; *SEISMIC EXPLORATION; *SEISMIC RECORDING; *SEISMIC REFLECTION METHOD; *THREE COMPONENT RECORDING; *VERTICAL SEISMIC PROFILING; ACCELEROMETER; BOREHOLE; CASINGS; CHART; CONNECTOR; COUPLING (MECHANICAL); DATA; DATA ACQUISITION; DEEP HOLE GEOPHONE; FINITE ELEMENT; FITTING; FREQUENCY; GEOPHYSICAL DATA; GRAPH; HARRIS CO, TEX; HUMBLE OIL FIELD; INSTRUMENT; MATHEMATICS; NOISE; NORTH AMERICA; PHOTOGRAPH; PIEZOELECTRIC GEOPHONE; PRESSURE; REFLECTION (SEISMIC); SEISMIC DATA; SEISMIC NOISE; SEISMIC WAVE PROPAGATION; SIGNAL TO NOISE RATIO; SONDE; SUBSURFACE PRESSURE; SUBSURFACE TEMPERATURE; TEMPERATURE; TEXAS; TRANSMISSION (SEISMIC); UNITED STATES; WAVE FREQUENCY; WAVE PHENOMENON; WAVE PROPAGATION; WESTERN US
 MH - *THREE COMPONENT GEOPHONE
 CC - GEOPHYSICS
 AB - AN ADVANCED 3-COMPONENT BOREHOLE SEISMIC RECEIVER HAS BEEN DESIGNED, DEVELOPED AND TESTED. THIS RECEIVER WAS DESIGNED WITH THE AID OF FINITE ELEMENT VIBRATION MODELING TO BE FREE OF SIGNIFICANT CLAMP RESONANCES BELOW 2,000 HZ. THIS BROAD FREQUENCY RANGE MAKES THIS SONDE WELL SUITED FOR CROSS-Well SEISMIC IMAGING APPLICATIONS. STATE-OF-THE-ART PIEZOELECTRIC ACCELEROMETERS ARE USED AS THE 3-COMPONENT SENSORS AND PROVIDE SIGNAL ENHANCEMENT RELATIVE TO CONVENTIONAL GEOPHONES. THE USE OF THESE ACCELEROMETERS OFFER A SIGNAL-TO-NOISE ENHANCEMENT OF APPROX. 20 DB AT 1,000 HZ OVER MOVING-COIL SEISMIC GEOPHONES. A PROTOTYPE ACCELEROMETER-BASED SONDE WAS FIELD TESTED AT THE TEXACO HUMBLE FIELD TO DETERMINE ITS PERFORMANCE CHARACTERISTICS. THE ADVANCED SONDE EXHIBITED SIGNIFICANTLY IMPROVED COUPLING RELATIVE TO THE VSP (VERTICAL SEISMIC PROFILE) TOOL AS EVIDENCED BY INCREASED BANDWIDTH AND SIGNAL-TO- NOISE RATIO. ADDITIONALLY, THE ADVANCED SONDE PRODUCED SIGNALS WHICH RIVAL THOSE PRODUCED BY THE BURIED/CEMENTED GEOPHONES.

PY - 91

SS 7?

improve (s) coupling (s) three-component (s) seismic (s) sensor

OCCURS	TERM
7049	IMPROVE
14432	COUPLING
0	THREE-COMPONENT
65881	SEISMIC

9432 SENSOR
SS 7 RESULT (0)

SS 8?
improve (s) coupling (s) vsp

OCCURS	TERM
7049	IMPROVE
14432	COUPLING
1241	VSP

SS 8 RESULT (0)

SS 9?
improve (s) coupling (s) seismic

*SEARCHING

OCCURS	TERM
7049	IMPROVE
14432	COUPLING
65881	SEISMIC

SS 9 RESULT (2)

SS 10?
print scanplus 1-2

-1- (TULSA)
AN - 490607
TI - A NEW OCEAN BOTTOM SEISMOMETER
AU - SAUTER, A; CURRIER, R; DORMAN, L; HALLINAN, J H; WOODLING, B; SCHULTZ, A
PY - 90

-2- (TULSA)
AN - 399657
TI - THE ROLE OF SEISMIC IN PLAY TYPE AND PROSPECT DEVELOPMENT: EASTERN
CANNING BASIN
AU - JACOBSON, T
PY - 84

SS 10?

?

?

?

?

print full 1-2

-1- (TULSA)
AN - 490607
TI - A NEW OCEAN BOTTOM SEISMOMETER
AU - SAUTER, A; CURRIER, R; DORMAN, L; HALLINAN, J H; WOODLING, B; SCHULTZ, A
OS - SCRIPPS INST OCEANOGR; WOODS HOLE OCEANOGR INST; WASHINGTON UNIV
SO - MAR TECHNOL SOC MAR INSTRUM '90 CONF (SAN DIEGO, 90.02.27-3/1/90) PROC
PP
99-103, 1990 (5 REFS)
LA - ENGLISH
DT - (AT) MEETING PAPER TEXT
IT - *OCEAN BOTTOM SEISMOMETER; *COMPUTER CONTROL; *CONTROL; *DATA
ACQUISITION; *EXPLORATION; *GEOPHYSICAL EQUIPMENT; *GEOPHYSICAL
EXPLORATION; *INSTRUMENTATION; *MARINE EXPLORATION EQUIPMT; *SEISMIC
EQUIPMENT; *SEISMIC EXPLORATION; *SEISMIC REFRACTION METHOD;
*SEISMOMETER; *SYSTEM (ASSEMBLAGE); ACOUSTICS; ARRAY; BLOCK DIAGRAM;
BOOK; CHART; CODING; COMPUTER; COMPUTER PROGRAM LANGUAGE; COMPUTER
PROGRAMING; COMPUTER STORAGE; DATA; DATA ANALYSIS; DATA PROCESSING; DATA
RECORDING; DATA STORAGE; DESIGN; DESIGN CRITERIA; DIAGRAM; DIGITIZATION;
ELASTIC WAVE; ENGINEERING; ENGINEERING DRAWING; ENVIRONMENT; FLOW CHART;
FREQUENCY; FREQUENCY RESPONSE; GEOPHONE; GEOPHYSICAL DATA; GROUND
COUPLING; HORIZONTAL ARRAY; INSTRUMENT; LOW FREQUENCY; LOW FREQUENCY
RESPONSE; MICROPROCESSOR; MICROSEISM; MONITORING; OCEAN ENVIRONMENT;
OPTICAL INSTRUMENT; PATTERN; PHYSICAL PROPERTY; PROGRAMING; RECORDER;
RECORDING; REFRACTION (SEISMIC); REMOTE SENSING; RESPONSE; SEA FLOOR;
SEISMIC DATA; SEISMIC WAVE; SEISMIC WAVE PROPAGATION; SEISMICITY;
SOFTWARE; SPECIFICATION; TESTING; THREE COMPONENT GEOPHONE; WAVE; WAVE.
PHENOMENON; WAVE PROPAGATION
MH - *OCEAN BOTTOM SEISMOMETER
CC - GEOPHYSICS
AB - THE MARINE PHYSICAL LAB. AT SCRIPPS INST. OF OCEANOGRAPHY IN
CONJUNCTION WITH WOODS HOLE, MIT, AND THE UNIVERSITY OF WASHINGTON HAVE
DEVELOPED A NEW OCEAN BOTTOM SEISMOMETER (OBS) FOR THE PURPOSE OF
RECORDING SEISMIC AND ACOUSTIC SIGNALS BETWEEN .05 AND 60 HZ. THE SNAG
(SEAFLOOR NOISE ADVISORY GROUP) OBS DESIGN INCORPORATES A FUNCTIONALLY
VERSATILE, LOW-POWER C44 BUS MICROPROCESSOR CONTROLLER, AN EXTREMELY
ACCURATE, LOW-POWER SEASCAN CLOCK, AND A 400- MBYTE MAXTOR OPTICAL
RECORDER. GAIN RANGING INCREASES SIGNAL DYNAMIC RANGE TO 126 DB. THE
SNAG OBS IS MADE UP OF 3 PARTS: THE RECORDING PACKAGE, THE ACQUISITION
PACKATE, AND THE SENSOR PACKAGE. THE SENSOR PACKAGE IS DEPLOYED A SMALL
DISTANCE AWAY FROM THE REST OF THE OBS TO IMPROVE SEISMIC COUPLING WITH
THE SEAFLOOR. SEISMOMETER SIGNALS ARE SENT BY CABLE TO THE ACQUISITION
PACKAGE, WHERE THEY ARE FILTERED AND DIGITIZED BY A FAST, ACCURATE
16-BIT
LOW POWER A TO D. DATA ARE BUFFERED TO ALLOW FOR PRE-EVENT RECORDING.
TRIGGERED EVENT DATA AND SCHEDULED DATA BLOCKS ARE THEN SENT TO THE
RECORDING PACKAGE. BATTERY POWER ALLOWS DEPLOYMENTS UP TO 1.5 MO. ALL
INSTRUMENTS ARE LINKED TOGETHER ON SHIPBOARD TO A SINGLE TERMINAL.
PY - 90
-2- (TULSA)
AN - 399657
TI - THE ROLE OF SEISMIC IN PLAY TYPE AND PROSPECT DEVELOPMENT: EASTERN
CANNING BASIN
AU - JACOBSON, T

OS - RANGER OIL (AUSTRAL) LTD
SO - THE CANNING BASIN, WA (BOOK: ISBN 0-909869-37-5) GEOL SOC AUSTRAL INC,
PERTH; PP 121-134, 1984 (JOINT AUSTRAL GEOL SOC & PETROL EXPLOR SOC
AUSTRAL CANNING BASIN SYMP (PERTH, W AUSTRAL, 84.06.27-29) PROC)
NU - ISBN 0909869375) GEOL SOC AUSTRAL INC, PERTH
LA - ENGLISH
DT - (AT) MEETING PAPER TEXT
IT - *WESTERN AUSTRALIA; *AUSTRALIA; *CANNING BASIN; *COMPLEX FAULTING;
*DEFORMATION; *EXPLORATION; *FAULTING; *GEOLOGY; *GEOPHYSICAL
EXPLORATION; *OCEANIA; *REFLECTION (SEISMIC); *ROCK DEFORMATION;
*SEISMIC
EXPLORATION; *SEISMIC REFLECTION METHOD; *SEISMIC WAVE PROPAGATION;
*STRUCTURAL GEOLOGY; *WAVE PHENOMENON; *WAVE PROPAGATION; ANTICLINE;
BASIN; BASIN DEPOSIT; BASIN SHELF; BOOK; CARBONIFEROUS; CHART;
CONTEMPORANEOUS FAULTING; CORRECTION; DEPOSIT (GEOLOGY); DEVONIAN; EARTH
AGE; FAULT (GEOLOGY); FAULT BLOCK; FOLD (GEOLOGY); GEOLOGIC STRUCTURE;
GEOPHYSICAL INTERPRETATION; HISTORY; HORST; HYDROCARBON POTENTIAL; INDEX
MAP; INTERPRETATION; MAP; NORMAL FAULT; ORDOVICIAN; PALEOZOIC; PETROLEUM
INDUSTRY; PROFILE; RECONNAISSANCE SURVEYING; RECORD QUALITY; REFLECTING
BED; REFLECTION PROFILE; SEISMIC INTERPRETATION; SEISMIC PROFILE;
SEISMIC
RECORD QUALITY; SEISMIC WAVE SOURCE; STATIC CORRECTION; SURVEYING;
THRUST
FAULT; WAVE SOURCE
MH - *WESTERN AUSTRALIA
CC - GEOPHYSICS
AB - THE EASTERN PART OF THE CANNING BASIN COVERS AN AREA OF 125,000 SQ KM.
BECAUSE OF ITS REMOTENESS FROM THE COAST, THIS AREA REMAINED RELATIVELY
UNEXPLORED AS LATE AS 1980. THIS REMOTENESS, TOGETHER WITH POOR SEISMIC
DATA, HELD BACK THE IDENTIFICATION OF PLAY TYPES AND THE DEVELOPMENT OF
STRUCTURAL CLOSURES FOR DRILLING. ALTHOUGH THERE HAS BEEN A RELATIVELY
LARGE EXPLORATION EFFORT IN THE NORTH SINCE 1980, AMOUNTING TO 8,500 KM
OF SEISMIC AND 2 WELLS, A LARGE AREA STILL REMAINS UNEXPLORED. A LARGE
NUMBER OF COMPRESSIONAL AND EXTENSIONAL STRUCTURAL PLAY TYPES HAVE BEEN
IDENTIFIED FROM THE RECENT ROUND OF SEISMIC EXPLORATION. HOWEVER,
SEISMIC DATA QUALITY IS GENERALLY NOT SUITABLE FOR THE DETAILED MAPPING
OF STRATIGRAPHIC FEATURES. CLOSE ATTENTION TO STATICS ESTIMATION
PROCEDURES AND THE UTILIZATION OF THE SUMMER WET SEASON TO IMPROVE
SEISMIC COUPLING, ARE ESSENTIAL FOR ACQUIRING THE NECESSARY HIGH
RESOLUTION SEISMIC DATA.
PY - 84

SS 10?
plurality (s) seismic (s) wavefield

OCCURS	TERM
196	PLURALITY
65881	SEISMIC
765	WAVEFIELD

SS 10 RESULT (0)

SS 11?
common (s) cross (s) gather

OCCURS	TERM
12728	COMMON
54498	CROSS
637	GATHER

SS 11 RESULT (0)

SS 12?
transversely (s) polarized

OCCURS	TERM
742	TRANSVERSELY
404	POLARIZED

SS 12 RESULT (3)

SS 13?
print scanplus 1-3

-1- (TULSA)
AN - 581187
TI - ARRAY RETROREFLECTOR APPARATUS FOR REMOTE SEISMIC SENSING
AU - BERNI, A J
PY - 94

-2- (TULSA)
AN - 573721
TI - RETROREFLECTOR APPARATUS FOR REMOTE SEISMIC SENSING
AU - BERNI, A J
PY - 94

-3- (TULSA)
AN - 465722
TI - BOREHOLE WAVE PARTICLE MOTION IN ANISOTROPIC FORMATIONS
AU - LEVEILLE, J P; SERIFF, A J
PY - 89

SS 13?
logoff

OK? (Y/N/H)

Y

SESSION FINISHED 10/09/98 12:33 P.M. (CENTRAL TIME)
ELAPSED TIME ON TULSA: 0.35 HRS.
\$23.45 EST COST CONNECT TIME.
\$10.00 EST COST ONLINE PRS: 14
\$33.45 EST TOTAL COST THIS TULSA SESSION.

ELAPSED TIME THIS SESSION: 0.36 HRS.
\$23.91 EST COST CONNECT TIME.
\$4.68 EST COST TELECOM.
\$10.00 EST COST ONLINE PRS: 14
\$38.59 EST TOTAL COST THIS TERMINAL SESSION.

ORBIT SEARCH SESSION COMPLETED. THANKS FOR USING ORBIT!
Trying 01182...Open

PLEASE ENTER HOST PORT ID:
PLEASE ENTER HOST PORT ID:x
LOGINID:d280jrs
PASSWORD:

189170 TRANSVERSELY
31494 POLARIZED
6102 SEISMIC
L1 0 TRANSVERSELY (W) POLARIZED (W) SEISMIC

=> s plurality (w) seismic (w) wavefield

1035624 PLURALITY
6102 SEISMIC
192 WAVEFIELD
L2 0 PLURALITY (W) SEISMIC (W) WAVEFIELD

=> common (w) receiver (w) gather

'COMMON' IS NOT A RECOGNIZED COMMAND

=> s common (w) receiver (w) gather

630074 COMMON
130723 RECEIVER
11727 GATHER
L3 28 COMMON (W) RECEIVER (W) GATHER

=> s l3 and vertical (w) gather

632274 VERTICAL
11727 GATHER
1 VERTICAL (W) GATHER
L4 0 L3 AND VERTICAL (W) GATHER

=> d ti l3 1-28

US PAT NO: 5,818,795 [IMAGE AVAILABLE] L3: 1 of 28
TITLE: Method of reduction of noise from seismic data traces

US PAT NO: 5,774,417 [IMAGE AVAILABLE] L3: 2 of 28
TITLE: Amplitude and phase compensation in dual-sensor ocean
bottom cable seismic data processing

US PAT NO: 5,742,740 [IMAGE AVAILABLE] L3: 3 of 28
TITLE: Adaptive network for automated first break picking of
seismic refraction events and method of operating the
same

US PAT NO: 5,724,307 [IMAGE AVAILABLE] L3: 4 of 28
TITLE: Method for improving the coupling response of a
water-bottom seismic sensor

US PAT NO: 5,724,306 [IMAGE AVAILABLE] L3: 5 of 28
TITLE: Method for correcting dual sensor data for imperfect
geophone coupling using production seismic data

US PAT NO: 5,721,710 [IMAGE AVAILABLE] L3: 6 of 28
TITLE: High fidelity vibratory source seismic method with source
separation

US PAT NO: 5,719,821 [IMAGE AVAILABLE] L3: 7 of 28
TITLE: Method and apparatus for source separation of seismic
vibratory signals

US PAT NO:	5,715,213 [IMAGE AVAILABLE]	L3: 8 of 28
TITLE:	High fidelity vibratory source seismic method using a plurality of vibrator sources	
US PAT NO:	5,703,833 [IMAGE AVAILABLE]	L3: 9 of 28
TITLE:	One step inversion/separation scheme using a plurality of vibrator sources	
US PAT NO:	5,696,734 [IMAGE AVAILABLE]	L3: 10 of 28
TITLE:	Method and system for eliminating ghost reflections from ocean bottom cable seismic survey signals	
US PAT NO:	5,677,892 [IMAGE AVAILABLE]	L3: 11 of 28
TITLE:	Unaliased spatial trace interpolation in the f-k domain	
US PAT NO:	5,648,938 [IMAGE AVAILABLE]	L3: 12 of 28
TITLE:	Seismic data acquisition	
US PAT NO:	5,617,372 [IMAGE AVAILABLE]	L3: 13 of 28
TITLE:	Unaliased spatial trace interpolation in the f-k domain	
US PAT NO:	5,616,840 [IMAGE AVAILABLE]	L3: 14 of 28
TITLE:	Method for estimating the hydraulic conductivity of a borehole sidewall fracture	
US PAT NO:	5,550,786 [IMAGE AVAILABLE]	L3: 15 of 28
TITLE:	High fidelity vibratory source seismic method	
US PAT NO:	5,537,319 [IMAGE AVAILABLE]	L3: 16 of 28
TITLE:	Method for load balancing seismic migration processing on a multiprocessor computer	
US PAT NO:	H 1,529 [IMAGE AVAILABLE]	L3: 17 of 28
TITLE:	Method for wave equation velocity replacement of the low-velocity-layer in seismic data processing	
US PAT NO:	5,508,914 [IMAGE AVAILABLE]	L3: 18 of 28
TITLE:	Method for calculating static corrections for seismic data	
US PAT NO:	5,448,531 [IMAGE AVAILABLE]	L3: 19 of 28
TITLE:	Method for attenuating coherent noise in marine seismic data	
US PAT NO:	5,442,591 [IMAGE AVAILABLE]	L3: 20 of 28
TITLE:	Method for adaptively suppressing noise transients in summed co-sensor seismic recordings	
US PAT NO:	5,293,352 [IMAGE AVAILABLE]	L3: 21 of 28
TITLE:	Method for removing noise due to near surface scatterers	
US PAT NO:	5,260,911 [IMAGE AVAILABLE]	L3: 22 of 28
TITLE:	Seismic surveying	
US PAT NO:	5,181,171 [IMAGE AVAILABLE]	L3: 23 of 28
TITLE:	Adaptive network for automated first break picking of seismic refraction events and method of operating the same	
US PAT NO:	5,073,876 [IMAGE AVAILABLE]	L3: 24 of 28
TITLE:	Geophysical exploration using near surface structure corrections developed from common endpoint gather	

stacked traces

US PAT NO: 5,050,129 [IMAGE AVAILABLE] L3: 25 of 28
TITLE: Marine seismic data conditioning

US PAT NO: 4,937,794 [IMAGE AVAILABLE] L3: 26 of 28
TITLE: Seismic noise suppression method

US PAT NO: 4,910,716 [IMAGE AVAILABLE] L3: 27 of 28
TITLE: Suppression of coherent noise in seismic data

US PAT NO: 4,577,297 [IMAGE AVAILABLE] L3: 28 of 28
TITLE: Method for enhancing recorded marine seismic reflection
signals having undulating water bottom distortions

=> d all 13 4

5,724,307 [IMAGE AVAILABLE] Mar. 3, 1998 L3: 4 of 28
Method for improving the coupling response of a water-bottom seismic
sensor

INVENTOR: James E. Gaiser, Littleton, CO
ASSIGNEE: Western Atlas International, Inc., Houston, TX (U.S.
corp.)
APPL-NO: 08/838,885
DATE FILED: Apr. 14, 1997
INT-CL: [6] G01V 1/36
US-CL-ISSUED: 367/21; 181/401
US-CL-CURRENT: 367/21; 181/401
SEARCH-FLD: 367/15, 21, 24; 181/122, 401, 402
REF-CITED:

U.S. PATENT DOCUMENTS
5,163,028 11/1992 Barr et al. 367/21

OTHER PUBLICATIONS

Vertical Seismic Profile Sonde Coupling; James E. Gaiser, et al,
Geophysics, vol. 53, No. 2 (Feb. 1988); pp. 206-214, 18 Figures.
ART-UNIT: 221
PRIM-EXMR: Ian J. Lobo
LEGAL-REP: William A. Knox

ABSTRACT:

A receiver consistent deconvolution operator models the damped
oscillatory wavetrain that is related to geophone coupling to the water
bottom. The operator is a best-fitting function that endeavors to
describe the difference in coupling response between a well-coupled
in-line geophone relative to an imperfectly-coupled cross-line geophone.
The operator is applied to the cross-line signals to compensate the
signals for the distortion due to imperfect cross-line ground coupling.

3 Claims, 10 Drawing Figures

EXMPL-CLAIM: 1
NO-PP-DRAWING: 7

SUMMARY:

BACKGROUND OF THE INVENTION

1. Field of the Invention

This invention is concerned with improving the coupling response of a

multi-axis seismic sensor or geophone implanted on a water bottom with particular attention to the sensor whose axis of sensitivity is spatially polarized along the cross-line axis.

2. Discussion of Relevant Art

Although the basic principles of seismic exploration are well known, a brief tutorial exegesis of the geophysical problems to be addressed by this invention now will be presented.

Please refer to FIG. 1 where a line of seismic transducers 10.sub.0, 10.sub.1, 10.sub.2, . . . , 10.sub.s ($s=3, 4, \dots, n$, where n is a large integer) are shown laid on the bottom 12 of a body of water, 14 (which may be for example, the open ocean, a lake, a bay, a river, a reservoir) spaced-apart by a desired spacing such as 25 meters. For purposes of this disclosure, the transducers are multiaxial motion-sensitive devices. In this disclosure, the terms "sensor", "receiver", "geophone" are synonymous. The terms refer to a mechanical-motion transducer which measures particle velocity. It to be distinguished from a hydrophone which is a pressure transducer.

The sensors are mechanically and electrically coupled to an ocean-bottom cable 16, one or both ends of which may be marked at the water surface 11 by a buoy such as 18. In practice, the cable 16 may be hundreds or thousands of feet long to which are attached many hundreds of sensors. For 3-D areal surveys, a number of cables may be laid out parallel to each other in a wide swath.

Usually, the cables and sensors are laid out over the area to be surveyed by a cable-tender boat. At some later time, a service ship such as 20 visits designated stations and retrieves one or more cables such as 16 from the water bottom, the ends having been flagged by buoys as shown. Cable 16 includes a plurality of internally-mounted communication channels (not shown), that may be electrical, optical, or in some cases ethereal, for transmitting the sensor output signals to digital data-recording and data-processing channels of any well known type (not shown) in ship 20. Ship 20 is equipped with a precision navigation means such as a GPS receiver and may include a radar beacon 22 for ranging on a radar reflector 24 mounted on tail buoy 18 at the other end of cable 16.

An acoustic sound source is fired at selected shot locations which may be spaced apart by an integral multiple of the sensor spacings. Source 26 radiates wavefields such as generally shown by 28 and 30 to insonify subsurface earth layers such as 32, whence the wavefield is reflected back towards the surface as reflected wavefield 34. The sensors 10.sub.s intercept the mechanical earth motions, convert those motions to electrical signals and send those signals through the communication channels to the recording equipment in ship 20.

A wavefield may propagate along a direct travel path such as 36 or along reflected-ray travel paths such as 38, 38' and 38" to the respective sensors 10.sub.s. The recorded data are presented in the form of time-scale traces, one trace per sensor/shot. A collection of time-scale traces resulting from a single source activation (a shot) that insonifies a plurality of receivers, such as in FIG. 1, constitutes a common source gather. On the other hand, with reference to FIG. 5, a collection of time-scale traces as recorded by a single sensor 10.sub.s after insonification by a plurality of spaced-apart shots 26, 26', 26" constitutes a **common** **receiver** **gather**. The space between a shot location and the surface expression, 27, of sensor 10.sub.s is the offset.

Typically in 3-D operations ship 20 occupies a central location, interconnected with a plurality of receivers, while a second shooting ship (not shown) actually visits the respective designated survey stations to generate common receiver gathers. The practice is necessarily required in 3-D because the survey stations are scattered over a two-dimensional area rather than being restricted to a single line of profile.

FIG. 2 is a close-up, X-ray-like side view of a multi-axis motion sensor 10.sub.s. The sensitive axes may be vertical, unit 40; in-line, unit 42; cross-line, unit 44. Usually, the two horizontally-polarized sensors preferably respond to shear waves and the vertical sensor responds to compressional waves. In some cases a two-axis instrument may be used for detecting shear waves only, with the sensor units directionally polarized along orthogonal x and y axes.

The multi-axis units are customarily packaged in a single case and internally gimbal-mounted so as to become automatically aligned along their mutually orthogonal axes after deposition on the sea floor. For good and sufficient reasons, the case containing the sensor components is usually cylindrical. Cable 16 is relatively heavy. Secured to the fore and aft ends of the sensor case, the cable 16 firmly holds the multi-axis motion sensor to the sea floor 12. The in-line unit 42 is well coupled to sea floor 12 because it is oriented in the direction of the cable 16. In this direction, the area of contact with the sea floor is relatively large. Not so, the cross-line unit.

FIG. 3 is an X-ray-like cross section of multi-axial sensor 10.sub.s taken along line 3-3', looking back towards ship 20. Because of its cylindrical shape, case 10.sub.s not only rolls from side to side as shown by curved arrows 46, but water currents and other disturbances can cause the sensor to shift laterally in the cross-line direction as shown by arrows 48, 48'. Those disturbances do not affect the in-line units because of their respective polarizations but they do introduce severe noise to the cross-axis signals.

FIG. 4 is multi-axis sensor 10.sub.s as viewed from above along line 4-4' of FIG. 2. This Figure will be referenced again later.

A geophone as used on ocean-bottom cables is a spring-mass oscillatory system. Assuming perfect coupling, the transfer function of a geophone can be described in terms of damping, η , resonant or natural frequency, ω , and phase angle, ϕ , relative to an input step function. Customarily geophones are damped at about 0.7 of critical at a resonant frequency of about 10-20 Hz. Assuming use of a velocity phone, below the natural frequency, the attenuation rate is 12 dB per octave; well above the natural frequency, the response is substantially constant within the useful seismic frequency band. The phase response may be non-linear below the resonant frequency and lags about 90.degree. behind the input transient above that value. Other signal distortions may be superimposed on the sensor output signals due to the respective transfer functions characteristic of the data transmission channels and the data processing equipment.

Instrumental response parameters can, of course be predicted on the basis of design criteria. But an imperfect earth-coupling response cannot be predicted. Multi-axis seismic sensors are essential for use in shear-wave surveys where, for example, in-line and cross-line shear waves are resolved to measure the azimuth of substantially-vertical formation fracturing. It is evident that if the cross-line sensor response is

distorted relative to the in-line sensor response, the resulting azimuth determination will be flawed. Resource-exploitation operations premised on flawed data is doomed to economic catastrophe.

A method for correcting poor coupling of a logging sonde in a borehole was described in a paper by J. E. Gaiser et al., entitled Vertical Seismic Profile Sonde Coupling, published in Geophysics n. 53, pp 206-214, 1988. However that method is not directly applicable to 3-D seismic exploration. There is a long-felt need for a method for measuring and suppressing signal distortion attributable to poor water-bottom coupling of one of the components of a cable-mounted, multi-axial sensor.

SUMMARY OF THE INVENTION

This is a method for removing objectionable ground-coupling response characteristics from seismic signals due to an imperfect ground coupling of a seismic receiver that is polarized in the cross line direction relative to a well-coupled, co-located seismic receiver polarized in the in-line direction. Along a preselected source-receiver trajectory vector, a plurality of in-line seismic-signal wavetrains emanating from an in-line receiver is assembled into a first common-receiver trace gather. Similarly a plurality of cross-line seismic-signal wavetrains emanating from a seismic receiver that is co-located with the in-line receiver are gathered in a second common-receiver trace gather. Each of the seismic-signal wavetrains resident in the respective first and second common-receiver trace gathers is auto-correlated in the time domain to provide a plurality of in-line and cross-line auto correlations. The respective in-line auto-correlations are normalized to unity and the respective cross-line auto-correlations are normalized to the corresponding in-line auto-correlations. The normalized cross-line auto-correlations are scaled to compensate for the difference between the cross-line polarization direction and the pre-selected source-receiver trajectory vector. The normalized in-line auto-correlations and the normalized, scaled cross-line auto-correlations are averaged and the averages are transformed to the frequency domain to define in-line and cross-line amplitude spectra. The cross-line auto-correlation is deconvolved by the in-line auto-correlation to define a coupling deconvolution operator. The coupling deconvolution operator is applied to the cross-line seismic-signal wavetrains resident in the cross-line common-receiver trace gather to remove the imperfect ground-coupling response characteristics from the cross-line receiver signals.

DRAWING DESC:

BRIEF DESCRIPTION OF THE DRAWINGS

The novel features which are believed to be characteristic of the invention, both as to organization and methods of operation, together with the objects and advantages thereof, will be better understood from the following detailed description and the drawings wherein the invention is illustrated by way of example for the purpose of illustration and description only and are not intended as a definition of the limits of the invention:

FIG. 1 is a conventional view of a ship servicing an ocean-bottom cable to which are coupled a plurality of multi-axis sensors;

FIG. 2 is an X-ray-like cross section of a three-axis seismic sensor;

FIG. 3 is an end view of the three-axis seismic sensor;

FIG. 4 is a view of the three axis sensor of FIG. 2 as seen from above;

FIG. 5 illustrates the concept of common receiver gathers;

FIG. 6 is a panel showing an in-line gather of seismic signals in comparison with a cross-line gather of seismic signals showing the effects of poor cross-line ground coupling;

FIG. 7 are the amplitude spectra of the in-line and the cross-line auto-correlations;

FIG. 8 show the ratio between the in-line and cross-line responses and the best-fitting estimate of the coupling response;

FIG. 9 is the phase response of the best-fitting estimate of FIG. 8;

FIG. 10 is the panel of FIG. 6 after compensation for imperfect ground-coupling response of the cross-line receiver.

DETDSC:

DETAILED DESCRIPTION OF THE PREFERRED EMBODIMENT

A deconvolution operator is desired that forms a receiver-consistent model of a damped oscillatory system that best describes the cross-line geophone coupling to the sea bed relative to that of a (theoretically) perfectly-coupled in-line sensor. The coupling response is then removed from the cross-line signals. It is assumed that the instrumental response characteristics are common to both receivers and are of no concern for purposes of this disclosure.

At a first receiver station, a first common receiver gathers of seismic signal traces are assembled, from an in-line receiver, $x_{sub.s}$, and a second ****common** **receiver** **gather**** of seismic signal traces from a co-located cross-line receiver, $y_{sub.s}$. The signals derive from many source stations areally distributed over the three-dimensional volume of the region of interest.

FIG. 6 is a panel showing first and second (counting from the left) in-line common trace gathers and third and fourth cross-line common trace gathers. The first and third and the second and fourth gathers are co-located. On the cross-line gathers, the first arrivals are greatly attenuated and a high-amplitude 20-Hz ringing-type interference is present. The 20-Hz interference is believed due to imperfect earth coupling.

Source-receiver data pairs are selected having a source-receiver trajectory vector along an azimuth that is about 45.degree., \pm some angular tolerance, to the mutual axial alignment of both of the horizontally-polarized receivers such as shown by the vectors 52 or 54, FIG. 4. Those data should therefore possess roughly equal signal levels in both components. It is preferable that a plurality of different source-receiver offsets, such as 0.0-500 meters be used over some preselected reflection-time window such as 3.0 seconds, counting from the first breaks.

Auto correlate each in-line source-receiver trace pairs of the ****common** **receiver** **gather**** as follows: **##EQU1##** Similarly, auto-correlate the cross-line source-receiver trace pairs: **##EQU2##** where the in-line auto-correlations are normalized to unity and each cross-line auto correlations are normalized relative to its in-line companion. T is

the length of the time window, τ is the phase lag and $x_{\text{sub.s}}$, $y_{\text{sub.s}}$ are the trace-bin idents for the in-line and the cross-line traces.

The cross-line responses must be balanced by a scale factor χ to correct for the level of the signal projected into the cross-line direction:

$\chi = \text{vertline.1} / \tan(\theta_{\text{sub.s}} - \theta_{\text{sub.x}}) \cdot \text{vertline.3}$
 where $\theta_{\text{sub.s}}$ is the source-receiver azimuth and $\theta_{\text{sub.x}}$ is the orientation of the in-line receiver. The scaled auto-correlations $\phi_{\text{sub.yy}}$ scaled by χ and the in-line auto-correlations $\phi_{\text{sub.xx}}$ are then averaged $\Phi_{\text{sub.xx}}$ and $\Phi_{\text{sub.yy}}$. $\Phi_{\text{sub.xx}}$ represents an estimate of the source-receiver response, multiples of the geological response and earth attenuation. The $\Phi_{\text{sub.yy}}$ response is representative of essentially the same parameters but with the cross-line coupling response added.

The average response functions are transformed to the frequency domain to provide in-line and cross-line amplitude spectra as shown in FIG. 7 where the bold curve is the cross-line response. The spectral ratio, in the frequency domain, of the average cross-line response to the average in-line response is shown as the thin curve in FIG. 8. That curve was computed by deconvolving the cross-line response by the in-line response in the time domain. Specifically, the deconvolution operator is the inverse of $\Phi_{\text{sub.xx}}$, such that when it is convolved with $\Phi_{\text{sub.xx}}$, an impulse results from that operation. Convolution of that operator with $\Phi_{\text{sub.yy}}$ results in the thin curve of FIG. 8 after transformation to the frequency domain. If the average cross-line response, $\Phi_{\text{sub.yy}}$, were identical to $\Phi_{\text{sub.xx}}$, that response function would be an impulse with an otherwise flat response spectrum. The deconvolution could, of course be done on individual data pairs rather than on the average of the pairs, if desired.

It is now required to determine the mechanical coupling parameters of a damped oscillatory system that best fits the observed spectrum. The parameters are the resonant or natural frequency ω_0 and damping parameter η , which can be determined by any number of well-known methods, one of which is presented here by way of example but not by way of limitation. The damped oscillatory system describing the coupling response may take the form $\frac{1}{\sqrt{1-i\eta\omega}}$ where ω is the angular frequency and $i = \sqrt{-1}$. It can be shown that $\frac{1}{\sqrt{1-i\eta\omega}}$ where ω_0 is the frequency at which the peak occurs in FIG. 8. Substituting (5) into (4) at the peak frequency where $\omega = \omega_0$ and after a bit of algebraic manipulation, it can be shown that $\frac{1}{\sqrt{1-\eta^2}}$ where $\Phi_{\text{sub.yy}}(\omega_0)$ and $\Phi_{\text{sub.yy}}(0)$ are the values of the frequency spectrum of the average auto-correlations after deconvolution at the maximum frequency and DC respectively.

Equation (6) is solved iteratively for η , where the left hand side of (6) is greater than unity. Substituting η in (5) gives ω_0 . The bold curve in FIG. 8 is the best fitting damped oscillatory response for ω_0 and η .

The deconvolution operator is applied, by frequency domain division, to all of the cross-line geophone signal traces for a specific receiver station. FIG. 10 shows the results. The in-line signals are unchanged but the 20-Hz oscillatory response has been removed from the cross-line data panel. The phase effects of the cross-line coupling response as shown in FIG. 9 have been removed. The first-arrival transients on the cross-line

panel have been enhanced.

This invention has been described with a certain degree of specificity by way of example but not by way of limitation. Those skilled in the art will devise obvious variations to the examples given herein but which will fall within the scope and spirit of this invention which is limited only by the appended claims.

CLAIMS:

What is claimed is:

1. A method for removing objectionable ground-coupling response characteristics from seismic signals due to an imperfectly-coupled seismic receiver polarized in a cross-line direction, relative to a well-coupled, co-located seismic receiver polarized in an in-line direction, comprising:
along a preselected source-receiver trajectory vector, assembling a plurality of in-line seismic-signal wavetrains emanating from a selected in-line seismic receiver in a first ****common**-**receiver**** ****gather**** and assembling a plurality of cross-line seismic-signal wavetrains emanating from a co-located cross-line receiver in a second ****common**-**receiver**** ****gather****;
in the time domain, individually auto-correlating each of the seismic-signal wavetrains resident in the respective first and second common-receiver gathers to provide a plurality of in-line and cross-line auto correlations;
normalizing the respective in-line auto-correlations to unity and normalizing the respective cross-line auto-correlations to the corresponding in-line auto-correlations;
scaling the normalized cross-line auto-correlations to compensate for the difference between the cross-line polarization direction and the pre-selected source-receiver trajectory vector;
averaging the normalized in-line auto-correlations and the normalized, scaled cross-line auto-correlations and transforming same to the frequency domain to define in-line and cross-line amplitude spectra;
deconvolving the cross-line auto-correlation by the in-line auto-correlation to define a coupling deconvolution operator; and
applying the coupling deconvolution operator to the cross-line seismic-signal wavetrains resident in the cross-line ****common**-**receiver**** ****gather**** to compensate said signals for the imperfect ground-coupling response characteristics due to the cross-line receivers.
2. The method as defined by claim 1, wherein:
the source-receiver trajectory vector is selected to substantially equalize the signal levels of the in-line and the cross-line auto-correlations except for the effects on the signals due to the difference in the ground-coupling characteristics of the respective receivers.
3. The method as defined by claim 2, wherein:
the deconvolution is accomplished by frequency-domain division.

=> d all 13 5

INVENTOR: Frederick James Barr, Houston, TX
ASSIGNEE: Western Atlas International, Inc., Houston, TX (U.S.
corp.)
APPL-NO: 08/580,634
DATE FILED: Dec. 29, 1995
INT-CL: [6] G01V 1/38
US-CL-ISSUED: 367/15, 21; 181/110, 112
US-CL-CURRENT: 367/15; 181/110, 112; 367/21
SEARCH-FLD: 367/15, 20, 21, 177, 178; 181/110, 112, 401
REF-CITED:

U.S. PATENT DOCUMENTS

4,253,164	2/1981	Hall, Jr.	367/22
5,365,492	11/1994	Dragoset, Jr.	367/21

ART-UNIT: 221
PRIM-EXMR: J. Woodrow Eldred
LEGAL-REP: Charles R. Schweppe

ABSTRACT:

A marine seismic surveying method recording with a first sensor a first signal indicative of pressure and with a second sensor a second signal indicative of motion, calculating a coupling mechanism filter for the second signal substantially correcting for the imperfect coupling of the second sensor, and applying a filter based on the coupling mechanism filter to at least one of the signals.

17 Claims, 7 Drawing Figures

EXMPL-CLAIM: 1
NO-PP-DRAWING: 6

SUMMARY:

BACKGROUND OF THE INVENTION

1. Field of the Invention

The present invention relates generally to marine seismic surveying and more particularly to a method for minimizing the effects of coupling differences between geophones and hydrophones in Dual Sensor bottom cables used in marine seismic surveying.

2. Description of the Related Art

Marine seismic surveying is a method for determining the structure of subterranean formations located beneath bodies of water. Marine seismic surveying typically employs survey ships, which are equipped with energy sources, and receiving ships, which are equipped with seismic receivers. The energy sources produce compressional seismic waves which propagate through the water and into the subterranean formations below. Different formation layers typically have different acoustic impedances, since the impedance is the product of varying rock density and wave velocity. Thus a portion of the waves will reflect up from the interfaces between adjacent formation layers. The reflected waves propagate back up through the earth and through the overlying water. The seismic receivers in the water convert the passing reflected waves into electrical or optical signals which are typically recorded and then processed into information about the structure of the subterranean formations. The reflected waves continue upward and a portion may continue to reflect back and forth between the water surface and the earth below. These additional reflections are also detected by the seismic receivers and cause noise that obscures the desired data. These unwanted reflections between the top and bottom of the water layer are called water column reverberations.

Energy sources commonly used in marine seismic surveying are air guns and marine vibrators. Air guns discharge air quickly under very high pressure into the water. The discharged air forms a seismic shock wave which contains frequencies within the seismic range. Marine vibrators actuate an acoustic piston to vibrate at a selected range of seismic frequencies. Both air guns and marine vibrators produce seismic waves of pressure differentials which propagate through the water and into the subterranean formations below.

Seismic receivers commonly used in marine seismic surveying are pressure sensors and motion sensors. Pressure sensors, such as hydrophones, convert pressure changes which accompany compressional seismic waves into electrical or optical signals which are recorded for analog or digital processing. Hydrophones typically employ a piezoelectric element to convert the pressure changes into electrical or optical signals. Motion sensors, such as geophones, convert particle velocities which accompany compressional seismic waves into electrical or optical signals. Geophones typically employ an electrical coil suspended relative to a magnet to convert vertical movement into electrical or optical signals. Less commonly used as receivers in marine seismic surveying are accelerometers. Accelerometers convert particle accelerations which accompany compressional waves into electrical or optical signals.

The ocean bottom cable method uses seismic sensor units which are attached to cables and deployed from seismic survey boats to rest on the marine bottom and record seismic data. The ocean bottom cable method is employed in relatively shallow water where nearby obstructions preclude the use of a towed streamer cable. The Dual Sensor method uses seismic sensor units which each contain both a pressure sensor and a motion sensor, usually a hydrophone and a geophone, respectively. The seismic signals from the hydrophone and the geophone are combined during processing to attenuate the effect of water column reverberations. Although hydrophones are typically used in marine operations, geophones are normally used in land operations. On land the geophones are anchored to the ground by metal spikes to ensure fidelity of geophone motion to land motion. Additionally, anchoring keeps the geophones oriented closer to vertical, which ensures a better measuring of vertical motion. In marine operations, however, anchoring the geophones to the solid earth of the ocean bottom with spikes is economically impractical. Instead, the geophones are normally mounted in gimbal mechanisms in the sensor units, which are attached to the bottom cable. The seismic survey ship deploys the bottom cable onto the ocean bottom, where the geophones lie suspended within the gimbal mechanisms inside the sensor units. The gimbal mechanisms orient the geophones vertically for proper operation.

The seismic signals from the hydrophone and the geophone in the Dual Sensor unit are typically combined during processing to attenuate the effect of water-column reverberations. Thus ideally the mechanical and electrical response of each type of receiver should match. A matching response would ensure that differences between the respective signals were due to differences in the physical properties being measured rather than to differences in the sensors. However, the response of the two sensors in a bottom cable operation do differ. One reason for the difference in sensor response is the difference in how the two types of sensors are coupled to the medium in which the physical changes being measured by the sensors take place. Hydrophones are sensitive to pressure changes in the water in which the hydrophones are immersed. Thus hydrophones are well coupled to the environment. The signals detected with hydrophones substantially correspond to the pressure being measured. However, physically coupling geophones to the ocean bottom is economically impractical, except by gravity. Thus geophones are

imperfectly coupled to the environment. The signals received from geophones do not always closely correspond to the vertical particle motion being measured. The imperfect coupling mechanism of the geophone must be corrected to match the response of the geophone to the response of the hydrophone for proper combining to attenuate water column reverberations.

F. J. Barr et al., Attenuation of Water Column Reverberations using Pressure and Velocity Detectors in a Water-Bottom Cable, 59th Annual Internat. Mtg., Soc. Expl. Geophys., Expanded Abstracts, 655, 1989, describes the theory of using both geophones and hydrophones to attenuate water-column reverberations. F. J. Barr, U.S. Pat No. 4,979,150, assigned to the assignee of the present invention, describes a method for using both geophones and hydrophones to attenuate water-column reverberations.

G. M. Hoover et al., The Influence of the Planted Geophone on Seismic Land Data, Geophysics, 45, 1239-1253, 1980, describes the physics of geophone ground coupling and some laboratory measurements of ground coupling with land geophones. C. E. Krohn, Geophone Ground Coupling, Geophysics, 49, 722-731, 1984, expands upon the Hoover et al. article and describes laboratory and field test measurements of ground coupling with land geophones.

Maxwell, P. W. et al., Recording Reliability in Seismic Exploration as Influenced by Geophone-Ground Coupling, 56th Mtg. and Tech. Exhib., EAEG, Expanded Abstracts, B014, 1994, describes a method of attaching a piezoelectric crystal device to a land geophone and applying an electric voltage to the crystal to tap the geophone. The response of the geophone to the tap is compared with the response of the geophone when coupling to the ground is known to be good. A filter can then be computed and applied to correct for less than optimum geophone to ground coupling.

F. J. Barr et al., U.S. Pat. No. 5,516,302 and U.S. Pat. No. 5,235,554, both patents assigned to the assignee of the present invention, describe a method of using information from a separate seismic data set called calibration shooting to determine the geophone coupling filter, along with other response differences between hydrophones and geophones.

None of the above articles or patents disclose a method using standard seismic equipment and production seismic data for correcting the effects of imperfect coupling of the geophone to the ocean bottom. Failure to correct for the response differences between the two types of sensors in the Dual Sensor method compromises the effectiveness of the attenuation of water column reverberations that can be achieved.

SUMMARY OF THE INVENTION

The present invention is a method for enhancing the effectiveness of marine surveying using a Dual Sensor ocean bottom cable. A first sensor generating a first signal indicative of pressure and a second sensor generating a second signal indicative of motion are deployed on the bottom of a body of water. A coupling mechanism filter is calculated for the second signal to correct for the imperfect coupling of the second sensor to the water bottom. A filter derived from the coupling mechanism filter is then applied to one of the signals to equalize the response of the two sensors.

DRAWING DESC:

BRIEF DESCRIPTION OF THE DRAWINGS

A better understanding of the benefits and advantages of the present invention may be obtained from the appended detailed description and drawing figures, wherein:

FIG. 1 is a diagrammatic view of marine seismic surveying utilizing the Dual Sensor ocean bottom cable method;

FIG. 2 is a diagrammatic view of a geophone and the geophone coupling mechanism;

FIG. 3 is a schematic diagram of the preferred method of the present invention;

FIG. 4 is a schematic diagram of an alternative embodiment of the method of the present invention;

FIG. 5 is an example of the series of p-traces generated by the method of the present invention for data from a survey in the Gulf of Mexico;

FIG. 6 is an example of the series of p-traces generated by the method of the present invention for data from a survey in offshore Gabon; and

FIG. 7 is an example of the series of p-traces generated by the method of the present invention for data from a survey in Lake Maracaibo, Venezuela.

DETDESC:

DESCRIPTION OF THE PREFERRED EMBODIMENTS

FIG. 1 shows a view of marine seismic surveying utilizing the Dual Sensor ocean bottom cable method. The bottom cable method employs a seismic survey ship 10 adapted for towing a seismic energy source 12 through a body of water 14. The seismic energy source 12 is an acoustic wave generating source, preferably an air gun. The bottom cable method typically also includes a receiving ship 16, preferably anchored in the body of water 14. The receiving ship 16 deploys a bottom cable 18 or a plurality of bottom cables 18 on the marine bottom 20. Each bottom cable 18 carries at least one Dual Sensor unit 22, but preferably carries a plurality of Dual Sensor units 22. Each Dual Sensor unit 22 contains a pressure sensor, preferably a hydrophone, and a motion sensor, preferably a geophone.

According to preferred practice, the receiving ship 16 or a separate cable handling ship (not shown) positions the bottom cable 18 with Dual Sensor units 22 on the marine bottom 20. The survey ship 10 typically moves at a constant speed along a predetermined path, such as a swath of parallel lines. The survey ship 10 generates seismic waves with the energy source 12 at predetermined locations along the path. After the survey ship 10 traverses each path, the receiving ship 16 or a separate cable handling ship retrieves the bottom cable 18 from the marine bottom 20. The receiving ship 16 or separate cable handling ship redeploys the bottom cable 18 at a new location, such as a line spaced from and parallel to the previous location of the bottom cable 18. The survey ship 10 then traverses another path, generating seismic waves with the energy source 12 at a new set of predetermined locations. The signals from the arrays of hydrophones and geophones are continuously recorded while the survey ship 10 fires the seismic energy source 12 at predetermined locations.

As the seismic energy source 12 generates seismic waves, a portion of the waves travel downward, as indicated by rays 30. A portion of the downward-traveling seismic waves are reflected up from interfaces between layers in the subterranean earth formations 40, such as interface 42 between layers 44 and 46, as illustrated. The reflected waves travel upwardly, as illustrated by rays 32. The sensors in the Dual Sensor units 22 in the bottom cable 18 detect the reflected waves as the waves travel upward past the locations of the Dual Sensor units 22 on rays 32. The pressure and motion sensors in the Dual Sensor Units 22 generate electrical or optical signals representative of pressure and particle velocity changes in the wave field and transmit the generated electrical or optical signals back to the receiving ship 16 via the cable 18. The recording equipment (not shown) within the receiving ship 16 records the electrical or optical signals so that the signals can be processed to map the subterranean formations 40.

The upward-travelling reflected waves reach the surface 24 of the body of water 14, where a portion of the waves are reflected back downward, as illustrated by rays 34. Each of the sensors in the Dual Sensor units 22 again detects the reflected waves as the waves travel downward past the locations of the Dual Sensor units 22 on rays 34. The reflected waves may continue to reverberate back and forth between the water bottom 20 or subterranean formations 40 below and the water surface 24 above. The multiply-reflected waves reverberating through the water layer will be detected by the sensors in the Dual Sensor units 22 at each pass, but carry no useful information about the subterranean formations 40. Rather, the reverberating waves act as noise, obscuring the information-carrying signals from the first reflections off the formation 40 interfaces. The noise-generating waves are called water column reverberations.

FIG. 2 shows a diagrammatic view of a geophone 70 and the coupling mechanism 72 of the geophone 70 to the ground 20. The geophone 70 comprises a geophone coil 74 of mass $m_{sub.g}$ suspended from a spring 76 inside a geophone case 80 of mass $m_{sub.c}$. The geophone coil 74 acts as a classical damped harmonic oscillator, coupled to the geophone case 80 by a spring 76 with spring constant $K_{sub.g}$ and a dashpot 78 with damping coefficient $B_{sub.g}$. The imperfect coupling 72 of the geophone 70 to the ground 20 acts as a filter on the seismic signal from the geophone 70. The filtering effect of the imperfect geophone coupling mechanism 72 is a damped, second-order system, as shown in C. E. Krohn, Geophone Ground Coupling, Geophysics, 49, 722-731, 1984. The coupling mechanism 72 is a classical damped harmonic oscillator. Thus the geophone case 80 acts as a damped harmonic oscillator coupled to the ground 20 by an additional spring 82 with spring constant $K_{sub.c}$ and an additional dashpot 84 with damping coefficient $B_{sub.c}$. The response of the geophone coupling mechanism 72 as a harmonic oscillator depends upon the natural resonance frequency $f_{sub.c}$ and damping coefficient $\zeta_{sub.c}$ of the geophone coupling mechanism 72. The two variables $f_{sub.c}$ and $\zeta_{sub.c}$ are functions of the elastic constants of the ground 20 and the total mass of the Dual Sensor unit containing the geophone 70. The mass of the Dual Sensor unit is typically much greater than the mass of a land geophone 70 because of the additional mass of both the gimbal mounting mechanism and the hydrophone contained within the Dual Sensor unit. The gimbal mechanism is required to orient the geophone 70 vertically when the Dual Sensor unit comes to rest on the ocean bottom 20. The increased mass of the Dual Sensor unit and the lack of a spike to anchor the geophone 70 to the ground 20 cause the natural resonance frequency of the geophone coupling mechanism 72 to be much lower than the range measured by C. E. Krohn, Geophone Ground Coupling, Geophysics, 49, 722-731, 1984, for land geophones 70. As a result, the filtering effect on the reflection wavelets is even greater for geophones 70 in marine operations than in

land operations.

The particle velocity manifestation accompanying the seismic waves causes the Dual Sensor unit and, therefore, the geophone case 80, to move in a vertical direction. The vertical component of the motion of the geophone case 80 is detected by the geophone 70 and results in a voltage wavelet which is digitized and recorded. However, the wavelet recorded from the geophone 70 is different from the wavelet recorded from the hydrophone because of the filtering effect of the geophone coupling mechanism 72. Let x indicate the true movement of the marine bottom 20, $x_{\text{sub.c}}$ the movement of the geophone case 80 relative to the marine bottom 20, and $x_{\text{sub.g}}$ the movement of the geophone coil 74 relative to the geophone case 80. The geophone 70 does not directly measure the true motion velocity (dx/dt) of the marine bottom 20. Instead, the geophone 70 measures the velocity ($d[x_{\text{sub.c}} - x_{\text{sub.g}}]/dt$) of the geophone case 80 relative to the geophone coil 74, as altered by the geophone coupling mechanism 72.

Referring to FIG. 2, the total transfer function relating the geophone output voltage signal, $V_{\text{sub.out}}$, to the true ground velocity, (dx/dt), is derived here. Newton's second law applied to the balance of forces on two masses, the geophone coil 74 and geophone case 80, yields the following two equations, ##EQU1## Eq. (1) states that the sum of the forces acting on the geophone coil 74 is zero. Similarly, Eq. (2) states that the sum of the forces acting on the geophone case 80 is zero. Let X , $X_{\text{sub.c}}$, and $X_{\text{sub.g}}$ be the Laplace transforms, respectively, of the variables x , $x_{\text{sub.c}}$, and $x_{\text{sub.g}}$. Then the Laplace transforms of Eqs. (1) and (2) are, respectively, ##EQU2## Multiplying through and regrouping the negative terms in Eqs. (3) and (4) yields the following corresponding equations, ##EQU3## Factoring out the X , $X_{\text{sub.c}}$ and $X_{\text{sub.g}}$ variables in Eqs. (5) and (6) yields the following corresponding equations, ##EQU4## Solving Eqs. (7) and (8) for $X_{\text{sub.g}}$ and $X_{\text{sub.c}}$, respectively, yields ##EQU5## The output voltage, $V_{\text{sub.out}}$, of the geophone is proportional to the difference in velocity between the geophone coil 74 and the geophone case 80. Thus

$$V_{\text{sub.out}} = s(X_{\text{sub.c}} - X_{\text{sub.g}}). \quad (11)$$

Substituting the values for $X_{\text{sub.g}}$ and $X_{\text{sub.c}}$ from Eqs. (9) and (10), respectively, into Eq. (11) yields ##EQU6## Substituting the value for $X_{\text{sub.c}}$ from Eq. (10) again into Eq. (12) yields ##EQU7## The transfer function between the geophone's output voltage $V_{\text{sub.out}}$ and marine bottom velocity (dx/dt) is given by ##EQU8## Multiplying through, subtracting like terms, and dividing numerator and denominator by the product $m_{\text{sub.c}} \cdot m_{\text{sub.s}}$ in Eq. (14) yields the following result for the geophone transfer function, ##EQU9## In Eq. (16), each of the denominator's factors can be expressed in the form

$$s^2 + 2\zeta \omega_{\text{sub.n}} s + \omega_{\text{sub.n}}^2 \quad (17)$$

where

$\omega_{\text{sub.n}}$ = natural frequency,

ζ = damping coefficient.

So, analyzing Eq. (17) in terms of Eq. (16) gives the natural frequency $\omega_{\text{sub.g}}$ and damping coefficient $\zeta_{\text{sub.g}}$ for the geophone 70 as ##EQU10## Likewise, the natural frequency $\omega_{\text{sub.c}}$ and damping coefficient $\zeta_{\text{sub.c}}$ for the geophone coupling mechanism are given by ##EQU11## For the complex Laplace variable $s = \sigma + i\omega$, letting the real part $\sigma = 0$ gives $s = i\omega$, the Fourier transform. Here $\omega = 2\pi f$, which relates the natural frequency ω in radians to the natural frequency f in Hertz. Substituting for s in Eq. (16) gives the geophone transfer function as ##EQU12## Squaring and inverting Eq. (18) yields ##EQU13## Manipulating Eq. (19) and using Eq. (18) gives the

following relations for the geophone constants, ##EQU14## Likewise, the following relations hold for the coupling mechanism constants, ##EQU15## Substituting Eq. (25) through (28) into Eq. (24) yields a new form for the transfer function, ##EQU16## Since the natural frequencies in radians and Hertz are related by $\omega = 2\pi f$, the geophone transfer function as given by Eq. (2) can be written as ##EQU17## Here $\omega_{\text{sub.g}}$ $= 2\pi f_{\text{sub.g}}$ and $\omega_{\text{sub.c}}$ $= 2\pi f_{\text{sub.c}}$ define the natural frequencies $f_{\text{sub.g}}$ and $f_{\text{sub.c}}$ for the geophone 70 and the geophone coupling mechanism 72, respectively.

A similar expression for the hydrophone 60 transfer function may be derived as ##EQU18## Here $f_{\text{sub.h}}$ and $\zeta_{\text{sub.h}}$ represent the natural frequency and damping coefficient, respectively, for the hydrophone 60, while $f_{\text{sub.m}}$ and $\zeta_{\text{sub.m}}$ represent the natural frequency and damping coefficient, respectively, for the hydrophone coupling mechanism. The hydrophone 60 is well coupled to the water. Thus it is preferable to use an high value, such as $f_{\text{sub.m}} = 2000$ Hz, for the natural frequency of the hydrophone coupling mechanism in Eq. (31). Similarly, it is preferable to use the critical value, $\zeta_{\text{sub.m}} = 0.7$, for the damping coefficient of the hydrophone coupling mechanism in Eq. (31).

Taking a ratio of the geophone transfer function of Eq. (30) to the hydrophone transfer function of Eq. (31) yields the following expression ##EQU19##

FIG. 3 shows a schematic diagram of the preferred method of the present invention. Common-receiver-point (CRP) trace gathers are recorded, as shown in Block 100. A middle range of source-receiver offsets is selected for the seismic survey area, as shown in Block 102. Preferably, the range of offsets in Block 102 is selected to yield approximately 10 to 20 traces in each CRP gather from Block 100 having first-breaks refracted from a common subsurface horizon. Ten to 20 traces provide a sufficient number of traces to combine into a slant-stacked trace yielding a better signal-to-noise ratio than the individual traces, as will be discussed later.

For each CRP gather from Block 100, the traces in the hydrophone CRP gather falling in the range of offsets from Block 102 are selected, generating the hydrophone traces subset, as shown in Block 104. The traces in the geophone CRP gather which correspond to the traces in the hydrophone traces subset from Block 104 are selected, generating the geophone traces subset, as shown in Block 106. The first-break peaks of the traces in the hydrophone traces subset from Block 104 are selected, generating the set of first-break picks, as shown in Block 108. A least-mean-squared-error straight line in the x-t plane is fitted to the set of first-break picks from Block 108, generating the best-fit line, as shown in Block 110.

Any nonzero DC offset is removed from both the hydrophone traces subset from Block 104, as shown in Block 112, and from the geophone traces subset from Block 106, as shown in Block 114. The DC offset is the average of all the time sample values in each recorded seismic trace. Each of the hydrophone and geophone traces subsets is scanned for the respective highest-amplitude first-break peak. The traces in both the hydrophone and geophone traces subsets are scaled to equalize all the first-break peak amplitudes, as shown in Block 116 and Block 118, respectively. The signal-to-noise ratio of the individual traces can be improved by combining the traces in the traces subsets using a tau-p transform for a single value of p, i.e., a single slant. The tau-p transform is a Radon transform using straight lines, which generates a slant-stacked trace called a p-trace. After correcting for the static

deviation in each hydrophone trace, a hydrophone p-trace is generated from the scaled hydrophone traces subset from Block 116, as shown in Block 120. Similarly, a geophone p-trace is generated from the scaled geophone traces subset from Block 118, as shown in Block 122. The static deviations are indicated by the time offset between the set of first-break peaks for the hydrophone traces subset from Block 108 and the best-fit line from Block 110.

The Dual Sensor method combines hydrophone and geophone signals to attenuate the effects of water column reverberation. The present invention corrects for the imperfect geophone coupling mechanism to make the hydrophone and geophone signals similar enough for effective combination. Generating hydrophone and geophone p-traces yields traces representative of the hydrophone and geophone signals, but with better signal-to-noise ratios than the individual hydrophone and geophone traces. However, analysis of several data sets from various locations around the world reveals that the hydrophone and geophone p-traces generated in Blocks 120 and 122 are extremely dissimilar in the time period shortly after the first-break peaks from Block 108. The time at which the dissimilarity becomes extreme is typically 10 to 20 milliseconds after the first trough and the following peak in the amplitude of the first-breaks in the hydrophone traces. The dissimilarity between the hydrophone and geophone p-traces is greater than can be attributed to the effect of imperfect geophone coupling mechanism alone. Thus a window function is applied to limit the combining of the geophone and hydrophone signals to the time period in which the two signals are sufficiently similar after correction for the imperfect geophone coupling mechanism.

Two window functions have been found to work well. Let $t_{sub.1}$ be the time of the zero crossing between the first trough and the following peak on the hydrophone or geophone p-trace, whichever occurs later. Let $t_{sub.2}$ be the time of the next zero crossing after time $t_{sub.1}$ on the hydrophone or geophone p-trace, whichever occurs later. A preferred window function has a value of 1.0 from time $t=0$ seconds to the time $t_{sub.2}$. The preferred window function can be defined by ##EQU20## An alternative window function has a value of 1.0 from time $t=0$ seconds to the time $t_{sub.1}$. From that point in time forward, the value of the window function exponentially decays at a rate such that the value at the time $t_{sub.2}$ is e^{-2} . Thus the alternative window function can be defined by ##EQU21## The geophone p-trace from Block 122 is multiplied by the preferred window function of Eq. (33), as shown in Block 124. Alternatively, the geophone p-trace from Block 122 could be multiplied by the alternative window function of Eq. (34).

The ratio of geophone to hydrophone transfer functions derived earlier and given by Eq. (32) is applied to the non-windowed hydrophone p-trace from Block 120, as shown in Block 126. The ratio of transfer functions in Eq. (32) provides a measure of the relative effects of the hydrophone and geophone coupling mechanisms. Because the hydrophone is well coupled to the water, a natural frequency of $f_{sub.m} = 2000$ Hz and a damping coefficient of $\zeta_{sub.m} = 0.7$ for the hydrophone coupling mechanism are preferably used. The same window function used in Block 124 is applied to the hydrophone p-trace from Block 126, as shown in Block 128.

An iterative, multi-variable search for the geophone coupling mechanism filter which minimizes the mean-squared error between the geophone p-trace from Block 124 and the hydrophone p-trace from Block 128 is performed. The parameters varied in the search are the natural frequency $f_{sub.c}$ and damping coefficient $\zeta_{sub.c}$ of the geophone coupling mechanism. The search generates an optimum geophone coupling mechanism

filter, as shown in Block 130. A multidimensional downhill simplex method is preferably used to implement the search. A computer program for the downhill simplex method can be found in W. H. Press et al., Numerical Recipes in C, Cambridge University Press, 1992. Preferably, the optimum geophone coupling mechanism filter found in Block 130 is inverted and applied to all the traces in the original geophone CRP gather of Block 100, as shown in Block 132. Alternatively, the optimum geophone coupling mechanism filter found in Block 130 can be directly applied to all the traces in the original hydrophone CRP gather of Block 100.

If the signal-to-noise ratio of the individual hydrophone and geophone traces is acceptable, then generating the hydrophone and geophone p-traces is not required. FIG. 4 shows a schematic diagram of an alternative method of the present invention. Common-receiver-point (CRP) trace gathers are recorded, as shown in Block 150. For each CRP gather from Block 100, a hydrophone trace in the hydrophone CRP gather is selected, generating the hydrophone trace, as shown in Block 152. The corresponding trace in the geophone CRP gather is selected, generating the geophone trace, as shown in Block 154. The first-break peak of the hydrophone trace from Block 152 is selected, generating the first-break, as shown in Block 156. Nonzero DC offset is removed from both the hydrophone trace from Block 152, as shown in Block 158, and from the geophone trace from Block 154, as shown in Block 160. The geophone trace from Block 160 is multiplied by the preferred window function of Eq. (33), as shown in Block 162. Alternatively, the geophone trace from Block 160 can be multiplied by the alternative window function of Eq. (34).

The ratio of geophone to hydrophone transfer functions given by Eq. (32) is applied to the non-windowed hydrophone trace from Block 158, as shown in Block 164. A natural frequency of $f_{\text{sub.m}} = 2000$ Hz and a damping coefficient of $\zeta_{\text{sub.m}} = 0.7$ for the hydrophone coupling mechanism are preferably used. The same window function used in Block 162 is applied to the hydrophone trace from Block 164, as shown in Block 166.

An iterative, multi-variable search for the geophone coupling mechanism filter which minimizes the mean-squared error between the geophone trace from Block 162 and the hydrophone trace from Block 166 is performed. The parameters varied in the search are the natural frequency $f_{\text{sub.c}}$ and damping coefficient $\zeta_{\text{sub.c}}$ of the geophone coupling mechanism. The search generates an optimum geophone coupling mechanism filter, as shown in Block 168. Preferably, the optimum geophone coupling mechanism filter found in Block 168 is inverted and applied to all the traces in the original geophone CRP gather of Block 150, as shown in Block 170. Alternatively, the optimum geophone coupling mechanism filter found in Block 168 can be directly applied to all the traces in the original hydrophone CRP gather of Block 150.

Application of the method of the present invention to data from three Dual Sensor ocean bottom cable surveys is illustrated in FIGS. 5-7. FIG. 5 shows the series of p-traces generated by the method of the present invention for the Gulf of Mexico data. Trace 201 is the hydrophone p-trace constructed from the hydrophone traces subset. Trace 202 is the geophone p-trace constructed from the corresponding geophone traces subset. Trace 203 is the hydrophone p-trace 201 minus the geophone p-trace 202. Trace 204 and trace 205 are the hydrophone p-trace 201 and the geophone p-trace 202, respectively, with the preferred window function of Eq. (33) applied. Trace 206 is the windowed hydrophone p-trace 204 minus the windowed geophone p-trace 205. Trace 206 indicates the degree to which the attenuation of water column reverberations by the Dual Sensor method is compromised by the filtering effect of imperfect geophone coupling, even after trace scaling. Trace 207 is the hydrophone

p-trace 201 after application of the optimum geophone coupling mechanism filter followed by application of the preferred window function of Eq. (33). Trace 208 is a repeat of the windowed geophone p-trace 205. Trace 209 is the windowed, filtered hydrophone p-trace 207 minus the windowed geophone p-trace 208. Trace 210 is a repeat of the windowed hydrophone p-trace 206. Trace 211 is the geophone p-trace 202 after application of the inverse of the optimum geophone coupling mechanism filter followed by the preferred window function of Eq. (33). Trace 212 is the windowed hydrophone p-trace 210 minus the windowed, inversely filtered geophone p-trace 211. The amplitude of trace 212 is reduced from the amplitude of trace 206 by over 14 dB. The optimum parameters found for the geophone coupling mechanism were natural frequency $f_{sub.c} = 46.7$ Hz and damping coefficient $\zeta_{sub.c} = 1.36$.

FIG. 6 shows the same series of p-traces as FIG. 5 for data from a **common**-**receiver**-**gather** from a survey offshore Gabon. The improvement in Dual Sensor reverberation attenuation from use of the present invention is indicated by the reduction in amplitude of over 12 dB from trace 312 to trace 306. The optimum parameters found for the geophone coupling mechanism were natural frequency $f_{sub.c} = 25.5$ Hz and damping coefficient $\zeta_{sub.c} = 1.97$.

FIG. 7 shows the same series of p-traces as FIGS. 5 and 6 for a **common**-**receiver**-**gather** from a survey in Lake Maracaibo, Venezuela. The improvement in Dual Sensor reverberation attenuation from use of the present invention is indicated by the reduction in amplitude of almost 7 dB from trace 412 to trace 406. The optimum parameters found for the geophone coupling mechanism were natural frequency $f_{sub.c} = 27.3$ Hz and damping coefficient $\zeta_{sub.c} = 2.30$.

The present invention has been described with a certain degree of specificity. Variations will occur to those skilled in the art which are within the scope of the invention, which is limited only by the appended claims.

CLAIMS:

I claim:

1. A method of marine seismic surveying, comprising the steps of:
recording with a first sensor a first signal indicative of pressure and with a second sensor a second signal indicative of motion, said sensors deployed on a marine bottom;
calculating a coupling mechanism filter for said second sensor, said coupling mechanism filter substantially correcting for imperfect coupling of said second sensor to said marine bottom, by calculating a first transfer function for said first signal, calculating a second transfer function for said second signal, taking the ratio of said second transfer function to said first transfer function, applying said ratio to said first signal, generating a third signal, and optimizing said coupling mechanism filter to minimize the difference between said second signal and said third signal; and
applying a filter based upon said coupling mechanism filter to at least one of said signals.
2. The method of claim 1, wherein said recording step comprises the steps of:
deploying an ocean bottom cable on the bottom of a body of water;
deploying on said ocean bottom cable a first sensor generating a first signal indicative of pressure in said water and a second sensor generating a second signal indicative of vertical motion of said bottom

and influenced by imperfect coupling of said second sensor to said bottom, wherein said second sensor is in close proximity to said first sensor;
generating a seismic signal in said body of water;
detecting said seismic signal with said first and second sensors; and
generating signals with said first and second sensors indicative of said seismic signal.

3. The method of claim 1, wherein said applying step comprises the step of:
applying the inverse of said coupling mechanism filter to said second signal.

4. The method of claim 1, wherein said applying step comprises the step of:
applying said coupling mechanism filter to said first signal.

5. The method of claim 1, wherein the optimizing step comprises the step of:
performing an iterative, multivariable search to minimize the mean-squared-error between said second signal and said third signal.

6. The method of claim 5, wherein the variables varied in said search are the natural frequency $f_{sub.c}$ and damping coefficient $zeta_{sub.c}$ of said second transfer function.

7. The method of claim 5, wherein said search is accomplished by a multidimensional, downhill simplex method.

8. The method of claim 1, wherein said first transfer function is given as a function of frequency f by ##EQU22## where $f_{sub.1}$ =natural frequency of said first sensor,
 $f_{sub.c}$ =natural frequency of said coupling mechanism of said first sensor,
 $zeta_{sub.}$ = damping coefficient of said first sensor,
 $zeta_{sub.c}$ =damping coefficient of said coupling mechanism of said first sensor.

9. The method of claim 1, wherein said second transfer function is given as a function of frequency f by ##EQU23## where $f_{sub.2}$ =natural frequency of said second sensor,
 $f_{sub.c}$ =natural frequency of said coupling mechanism of said second sensor,
 $zeta_{sub.}$ = damping coefficient of said second sensor,
 $zeta_{sub.c}$ =damping coefficient of said coupling mechanism of said second sensor.

10. The method of claim 8, wherein said natural frequency $f_{sub.c}$ of said coupling mechanism of said first sensor is 2000 Hz and said damping coefficient $zeta_{sub.c}$ of said coupling mechanism of said first sensor is 0.7.

11. The method of claim 1, further comprising the steps of:
applying a window function to said second signal before calculating said second transfer function; and
applying said window function to said third signal before calculating said first transfer function.

12. The method of claim 11, wherein said window function is given by ##EQU24## where t =time, and
 $t_{sub.2}$ =time of the latter of the zero crossings immediately following

the zero crossing between the first trough and the following peak on said first signal or said second signal.

13. The method of claim 11, wherein said window function is given by ##EQU25## where $t = \text{time}$,
t.sub.1 = time of the latter of the zero crossings between the first trough and the following peak on said first signal or said second signal, and
t.sub.2 = the time of the latter of the next zero crossings on said first signal or said second signal after said time t.sub.1.

14. The method of claim 1, further comprising the steps of:
generating a first traces subset by selecting a plurality of first sensor traces from said first signal;
generating a second traces subset by selecting the second sensor traces from said second signal corresponding to said selected first sensor traces;
selecting first-break peaks of said first traces subset;
fitting a least-mean-squared-error straight line in the x-t plane to said first break peaks in said first traces subset;
removing any DC offset from said first and second traces subsets;
scanning each of said first and second traces subsets for highest amplitude of the peaks of said first breaks;
scaling traces in each of said first and second traces subsets to equalize said amplitude of said first-break peaks;
generating a single slant-stacked trace from each of said first and second traces subsets using the slope of said least-mean-squared-error straight line; and
using said slant-stacked traces as said first and second signals in said calculating a coupling mechanism filter step.

15. The method of claim 14, wherein said generating said first traces subset step comprises the steps of:
selecting a middle range of source receiver offsets in the survey area with approximately 10 to 20 traces in each common-receiver-point trace gather having first-breaks refracted from a common subsurface horizon; and
generating said first traces subset by selecting said first sensor traces from said common-receiver-point trace gather falling in said offset range.

16. The method of claim 14, wherein said generating a single slant-stacked trace step comprises the steps of:
taking data samples from each of the traces in said first and second traces subset at the points where the traces intersect a line with the same slope as the slope of said least-mean-squared-error straight line;
averaging the values of said traces at said data samples; and
repeating said taking and said averaging steps for a plurality of said lines with the same slope as the slope of said least-mean-squared-error straight line.

17. The method of claim 1, further comprising the steps of:
selecting a first trace from said first signal;
generating a second trace by selecting the trace from said second signal corresponding to said selected first trace;
selecting first-break of said first trace;
removing any DC offset from said first and second traces; and
using said first and second traces as said first and second signals in said calculating a coupling mechanism filter step.

=> d all 13 16

5,537,319 [IMAGE AVAILABLE] Jul. 16, 1996 L3: 16 of 28
Method for load balancing seismic migration processing on a
multiprocessor computer

INVENTOR: Eric J. Schoen, Austin, TX
ASSIGNEE: Schlumberger Technology Corporation, Austin, TX (U.S.
corp.)
APPL-NO: 08/224,603
DATE FILED: Apr. 7, 1994
REL-US-DATA: Continuation-in-part of Ser. No. 160,123, Dec. 1, 1993,
abandoned.
INT-CL: [6] G06F 19/00
US-CL-ISSUED: 364/421
US-CL-CURRENT: 702/14
SEARCH-FLD: 364/421, 422; 395/929
REF-CITED:

U.S. PATENT DOCUMENTS

4,598,400	7/1986	Hillis
4,773,038	9/1988	Hillis et al.
4,827,403	5/1989	Steele, Jr. et al.
5,128,899	7/1992	Boyd et al.
5,148,406	9/1992	Brink et al.
5,150,331	9/1992	Harris et al.
5,198,979	3/1993	Moorehead et al.

FOREIGN PATENT DOCUMENTS

2236393	4/1991	United Kingdom
8800711	1/1988	World Intellectual Property Organization
9313434	7/1993	World Intellectual Property Organization

OTHER PUBLICATIONS

Vijay K. Madisetti et al., "Seismic Migration Algorithms Using The FFT Approach On The NCUBE Multiprocessor", ICASSP '88 : Acoustics, Speech & Signal Processing Conference, 1988, pp. 894-897.

Vijay K. Madisetti et al., "Seismic Migration Algorithms On Multiprocessors", ICASSP '88: Acoustics, Speech & Signal Processing Conference, 1988, pp. 2124-2127.

Brian Kelley et al., "High Speed Migration Of Multidimensional Seismic Data", ICASSP '91: Acoustics, Speech & Signal Processing Conference, 1991 pp. 1117-1120.

Deregowski, S. and Rocca, F., 1981. Geometrical optics and wave theory for constant-offset sections in layered media. I Geophysical Prospecting, 29, 374-387.

Hillis, W. Daniel and Tucker, Lewis W. The CM-5 Connection Machine: A Scalable Supercomputer, Communications of the ACM, Nov. 1993, vol. 36, No. 11, pp. 31-40.

United States Statutory Invention Registration, Berryhill et al., Reg. No. H482, Published Jun. 7, 1988.

Highnam, P. T. and Pieprzak, A. Implementation of a Fast, Accurate 3-D Migration on a Massively Parallel Computer, Proceedings of 61st Annual International SEG Meeting, Nov. 13, 1991, vol. 1, 338-340.

Meinardus, H. A. and K. L. Schleicher, Jul. 1993. 3-D time-variant dip moveout by the f-k method, Geophysics, vol. 58, No. 7, 1030-1041.

Reshef, M., Aug. 1991. Prestack depth imaging of three-dimensional shot gathers. Geophysics, vol. 56, No. 8, 1158-1163.

Reynolds, S. Jun. 1993. Parallel computing in seismic data processing. The Leading Edge, vol. 12, No. 6, 687-692.

International Preliminary Examination Report dated Aug. 2, 1995, PCT International Application No. PCT/US94/13704, Schlumberger Technology Corporation, filed Jan. 12, 1994.

ART-UNIT: 241
PRIM-EXMR: Donald E. McElheny, Jr.
LEGAL-REP: Charles D. Huston

ABSTRACT:

This invention provides a means for balancing the computational workload of individual processing nodes of a multiprocessor computer, such as a massively parallel processor (MPP), when executing a seismic migration program. Groups of prestack seismic traces are loaded into "input" nodes of the MPP. The "input" nodes examine the traces to determine which bins in the seismic survey are covered by the traces, and how many traces cover each bin. Each input node then broadcasts to all other nodes a description of the trace coverage. All nodes use the information in each broadcast to determine how many bins will be assigned to each "operator" node that will process the prestack data to produce poststack data. The bin assignment is designed to equalize the number of traces that each operator node processes. Thus, the invention provides a means for maximizing the efficiency with which an MPP can perform seismic migration processing, and is applicable to wide variety of MPPs and processing algorithms.

13 Claims, 16 Drawing Figures

EXMPL-CLAIM: 1
NO-PP-DRAWING: 14

PARENT-CASE:

This application is a continuation-in-part of U.S. patent application Ser. No. 08/160,123 filed Dec. 1, 1993, now abandoned.

SUMMARY:

TECHNICAL FIELD

This invention relates to seismic data processing on multiprocessor computers. In particular, the current invention relates to a method of balancing the computational load of Kirchhoff-style seismic migration processing across multiple processors on a multiprocessor computer.

BACKGROUND OF THE INVENTION

Seismic Acquisition & Processing

The Earth's subsurface can be imaged by a seismic survey, therefore, seismic data acquisition and processing are key components in geophysical exploration. In a seismic survey, elastic acoustic waves are generated by a source at the Earth's surface and the waves are radiated into the Earth's subsurface. For land seismic surveys, the usual source is dynamite or a seismic vibrator, while for a marine seismic survey the source is typically an airgun array.

As the waves radiate downward through the Earth's subsurface, they reflect and propagate upwards towards the surface whenever the subsurface medium changes. The upward reflections are detected by a number of receivers and the reflected data recorded and processed in order to image the subsurface. Interpretation of these acoustic images of the subsurface formation leads to the structural description of the subsurface geological features, such as faults, salt domes, anticlines, or other features indicative of hydrocarbon traps.

While two dimensional ("2D") seismic surveys have been conducted since the 1920's , three dimensional ("3D") seismic surveys have only recently become widely used. 3D surveys more accurately reflect the subsurface positions of the hydrocarbon traps, but are expensive and time consuming to acquire and process. For an offshore 3D data set covering a 20.times.20 km area, it costs about \$3 M dollars (1991 dollars) to acquire the data with another \$1 M dollars for data processing to transform the raw data into usable images. Because the cost of such a seismic survey is considerably less than the cost of drilling an offshore oil well, 3D seismic surveys are often worth the investment.

One common type of seismic survey is a marine survey, performed by boats in offshore waters. To record seismic data, a boat tows airguns (seismic sources) near its stern, and an up to 5 km long "streamer" containing hydrophones (seismic receivers) along its length. As the boat sails forward, it fires one source and receives a series of echoes into each seismic receiver. For each source-receiver pair, one prestack seismic trace is created. Each trace records sound waves that echo from abrupt acoustic impedance changes in rock beneath the ocean floor. Also recorded in a prestack trace, in a header section of the trace record, is information about the location of the source and receiver [Barry, Cavers, and Kneale, 1975]. Prestack traces are not associated with any particular area of the survey. Each echo that appears in a prestack trace is caused by a reflector that lies somewhere along, and tangent to, an elliptical path whose foci are the seismic source and receiver.

The spatial relationship between sources and receivers in a land seismic acquisition scenario differs from that described above; however, the present invention is unaffected by this.

A seismic survey is performed over a bounded region of the earth. This region is generally, but not necessarily precisely, rectangular. The survey area is partitioned into an array of bins. "Binning" is the assignment of traces to a survey array--usually a 12.5 by 25 meter rectangle. Any particular bin is located by its Cartesian coordinates in this array (i.e., by its row and column number). The ultimate output of the seismic survey is data that shows the location and strength of seismic reflectors in each bin, as a function of depth or time. This information cannot be deduced directly, but rather must be computed by applying numerous data processing steps to data recorded.

Although 3D marine surveys vary widely in size (1,000 to 100,000 km.sup.2), a typical marine survey might generate in excess of 40,000 data acquisition tapes. Data is accumulated at a staggering rate, about 1.5 million data samples every 10 seconds. A significant amount of time and money is spent in processing this enormous amount of data. The result of the seismic survey is thus an enormous amount of raw data indicative of reflected signals which are a function of travel time, propagation, and reflection effects. The goal is to present the reflected amplitudes as a function of lateral position and depth.

A typical marine seismic survey goes through three distinct sequential stages--data acquisition, data processing, and data interpretation. Data processing is by far the most time consuming process of the three. The acquisition time for a medium to large 3D marine seismic survey is in the order of two months. In addition to seismic data, navigation information is also recorded for accurate positioning of the sources and receivers. The resulting digital data must be rendered suitable for interpretation purposes by processing the data at an onshore processing center. The processing sequence can be divided into the following five processing steps.

1. Quality Control, filtering and deconvolution. This processing is applied on a trace basis to filter noise, sharpen the recorded response, suppress multiple echoes, and generally improve the signal-to-noise ratio. Most of these signal processing operations can be highly vectorized.
2. Velocity analyses for migration. This processing estimates the velocity of the subsurface formations from the recorded data by modeling the propagation of acoustic waves with estimated velocities and checking for signal coherence in the acquired data. It is similar to migration but is applied to a small section of the data cube.
3. 3D dip moveout correction and stacking. This processing step, generally the most input/output intensive part of the processing, (i) sums together several traces in order to eliminate redundancy and increase the signal-to-noise ratio, (ii) corrects for time delays that occur when the reflected signal is recorded by successive hydrophones that are located increasingly farther away from the energy source, and (iii) positions and orients the stacked data in accordance with the navigation information. After this processing step, the data is referred to as stacked data. This step normally constitutes on the order of a 100 to 1 reduction in data volume. Migration. This processing step, computationally the most intensive, relocates the position of reflected strata, that are recorded in time, to their correct position in depth.
5. Enhancement and filtering. This processing step is used to enhance the migrated data using digital filtering techniques.

The stacking process (step 3) reduces the amount of data to what is essentially a three dimensional array of numbers (i.e. a data cube) representing amplitudes of reflected seismic waves recorded over a period of time (usually 8 seconds). Such data cubes can be large, for example, a medium size 3D survey may produce cubes as large as 1000.times.1000.times.2000 of floating-point numbers.

The stacked data cube represents a surface recording of acoustic echoes returned from the earth interior and is not usually directly interpretable. The migration (or acoustic imaging process, step 4) is used to convert stacked data into an image or a map which can then be viewed as a true depth map cut out of the survey area.

Thus, migration is one of the most critical and most time consuming components in seismic processing is migration. Generally speaking, migration transforms the seismic data recorded as a function of time into data positioned as a function of depth fusing preliminary knowledge of the propagation velocities of the subsurface. In particular, migration moves dipping reflectors to their true subsurface position. Migration is typically performed on post stack seismic data to reduce the amount of processing time, but even so takes weeks of conventional supercomputer time for even medium size post stack seismic data cubes.

Many types of stacking and migration processes are well known. See, O. Yilmaz. 1987. Seismic Data Processing. Tulsa, Okla.: Society of Exploration Geophysicists. Usually, one poststack trace is associated with each bin. However, it is also possible to create multiple poststack traces per bin. For example, each such trace might contain contributions from prestack traces whose source-receiver separation falls within a specific range. (In this case, the bin is said to contain a common depth-point or common midpoint gather.)

Stacking programs create poststack data from prestack data by simple manipulation of prestack data. In general, a stacking program transforms each prestack trace exactly once. Migration programs create poststack

data from prestack data by more complicated, computationally intensive, manipulation of the same data. Migration programs transform each prestack trace a large number of times, requiring commensurately more computation than simpler stacking programs. Multiple prestack traces are transformed and added together and superimposed to create the one or more poststack traces associated with a bin.

One common approach to implementing migration computations is the Kirchhoff method. See, U.S. Pat. No. 5,198,979 Moorhead et al. See also, S. Derogowski and F. Rocca, 1981. Geometrical optics and wave theory for constant-offset sections in layered media. *Geophysical Prospecting*, 29, 374-387. Using the Kirchhoff approach to implement 3D Dip Moveout ("DMO"), a program transforms a prestack trace once for each bin that lies under a line drawn between the seismic source and receiver. This line is referred to as the "coverage" of the trace. Each transformed prestack trace is added, sample-by-sample, to incrementally create one or more the poststack traces in each bin. The signal-to-noise ratio of each poststack trace increases as the square root of the number of transformed prestack traces added together to form it.

The Kirchhoff approach is computationally expensive. Approximately 30 arithmetic operations (floating-point operations, or FLOPs) are required for each sample of each transformed trace in DMO. Given an average shot-receiver separation of 3 kilometers, a bin width of 12.5 meters, and 8 seconds worth of data in each trace acquired at 4ms/sample, this implies an average of approximately 10 million FLOPs per trace. A typical 20 km square marine survey using 12.5 meter wide, 25 meter tall bins contains perhaps 80 million prestack traces. The DMO process thus consumes approximately 800 trillion FLOPs. This computational expense motivates the implementation of migration programs such as DMO on some form of high-performance supercomputer, such as a massively parallel processor. See, Thinking Machines Corporation, 1993. *The Connection Machine CM-5 Technical Summary*. Such a processor is an attractive platform upon which to execute migration programs, because its performance scales up as its size increases; thus, the system can grow incrementally as the computational demand of the processing organization increases. See also, W. Daniel Hillis and Lewis W. Tucker, *The CM-5 Connection Machine: A scalable supercomputer*, *Communications of the ACM*, November 1993, Vol. 36, No. 11, pp 31-40.

Parallel Computation

FIG. 1 is an example of a multiprocessor parallel computer, specifically a massively parallel processor (MPP) such as the CM-5. In FIG. 1, an MPP 10 consists of 3 major components: (i) a disk storage system 12 whose capacity and data transfer rate can be scaled up as storage and data throughput requirements demand, (ii) a data and control communications network 14 that ties together the processors and the disk storage system, and (iii) a set of processing nodes 16 (see FIG. 2), each containing at least one processor 18, memory 20, and interface 22 to the data and control network 14. The capacity of the data network 14 (the amount of data it can transport in a given amount of time) scales as the number of nodes 16 increases. The size of the set of processing nodes 16 can be scaled up as computational requirements demand. On an MPP, processor nodes 16 can execute independently from one another; however, the control portion of the data and control communications network 14 provides a means by which all nodes 16 can synchronize their activities.

An MPP can improve the performance of computationally-intensive migration programs because it is possible to partition the work to be done and assign a part of it to each processor node 16. For this approach to scale as the size of the MPP 10 scales, the work partitions must be

truly independent of one another, such that no two processors share work. This is an expression of Amdahl's Law, which states that the maximum parallelization speedup possible is the inverse of the fraction of time an application spends performing serial computation. See, G. Fox et al., 1988. Solving Problems on Concurrent Processors, Vol. 1, page 57.

For example, in seismic migration processing, each bin in the survey area must be assigned to one and only one processor at any one time. Any attempt to assign the same bin to more than a single processor would require a serializing synchronization to guarantee proper results. Because DMO moves a large amount of data, the means by which data is moved between the disk storage system 12 and the memories 20 of the processing nodes 16 is especially important. In order to avoid implications of Amdahl's Law, the data must be moved in parallel as efficiently as possible. One type of disk storage system that satisfies this requirement is a RAID disk system. See, S. J. Lo Verso, M. Isman, A. Nanopoulos, W. Nesheim, E. D. Milne, and R. Wheeler. SFS: A parallel file system for the CM-5. In Proceedings of the 1993 Usenix Conference.

Another implication of Amdahl's Law is that the work partitions must be designed so that all nodes are required to perform equal amounts of computation. This latter requirement is referred to as load balancing. Kirchhoff DMO on a Multiprocessor

A scalable means to implement DMO on a multiprocessor computer is to: (i) load a set of prestack traces from the disk storage system 12 into the processing nodes 16, (ii) determine which bins in the survey area are covered by the union of all of the loaded traces, (iii) assign to each node 16 a portion of the survey area covered by the loaded traces, (iv) load from the disk system 12 into the appropriate nodes 16 the poststack traces from the covered bins, (v) apply the DMO operator to each loaded prestack trace in each processor to update the poststack traces, and (vi) write out the updated poststack traces from the nodes 16 to the disk system 12. U.S. patent application Ser. No. 08/160,123 filed Dec. 1, 1993 describes a method for inputting seismic data for processing on a multiprocessor computer.

The assignment of portions of the survey area to the nodes 16 must be non-overlapping. This satisfies the independence requirement for scalability on an MPP because each bin is independent of other bins. This also permits a disk I/O strategy that allows the poststack traces to be read from and written to the disk storage system 12 in parallel. This is important, because each poststack trace will typically be read in, updated, and written out many times during the processing of a prestack data set. Thus, the organization of the file on the disk storage system containing the poststack data and the strategy with which the data is read and written can strongly impact the efficiency of the DMO process.

However, a simple non-overlapping partitioning of bins does not in itself guarantee good performance. For example, if each node is a priori assigned the same number of bins to process, this approach will not in general achieve good load balancing. This is especially true when marine seismic data is being processed, due to the geometry with which the data is acquired.

FIG. 3 depicts a typical configuration of seismic sources and receivers in a marine seismic survey. A seismic acquisition vessel 30 sails forward towing a streamer cable 32 containing multiple seismic receivers 36 located at different points along the cable. Near the stern of the vessel is a pair of airguns 34, which are the seismic sources. With each firing of an airgun, a collection of prestack seismic traces are recorded,

one-trace from each receiver 36. For each trace and each bin 38 under the coverage of the, the DMO operator transforms the trace and adds it to the poststack trace associated with the bin. Since the streamer cable 32 follows in a nearly perfect straight line behind the vessel 30 parallel to the direction the vessel is sailing, the bins closest to the airguns 34 (called "near offset" bins) and under the streamer cable will be in the coverage of more traces than the bins closest to the last receiver 36 on the cable (called "far offset" bins).

The ratio of traces covering a so-called "near offset" bin to those covering a "far offset" bin will be equal to the number of uniquely located receivers 36 on the streamer cable. Typically, there are between 120 and 240 receivers on a cable. This means that a processor node 16 assigned to process a near-offset bin will have perhaps 240 times more work to do than a node assigned to a far-offset bin.

The preceding discussion considered only the processing of a single shot record (the set of traces recorded by all of the receivers from a single shot of an airgun). The load imbalance problem is further exacerbated when multiple shots are processed simultaneously, as is typically done when executing DMO on a multiprocessor computer. To see why this is so, consider that the acquisition vessel sails forward a short distance (typically 25 meters) between shots. As a result, the number of traces covering bins near the near-offset bin of the first shot in a set of shots is multiplied roughly by the size of this set; however, the coverage of the first far-offset bin is unchanged, since the receiver at the end of the streamer cable has now been towed beyond the bin.

A similar load imbalance will exist when processing land seismic data, which is typically sorted into collections of prestack traces associated with each receiver point in the survey. The corresponding shot points are located in all directions and at various distances from the receiver, causing the trace coverage of bins near the receiver to be higher than those farther from the receiver. If sets of traces from multiple receivers are processed simultaneously, and if the receivers in the set are located near one another, the severity load imbalance problem will increase, as it does when multiple marine shot gathers are processed.

In this application, all references to patents are incorporated by reference and all other references are incorporated by reference for background.

SUMMARY OF THE INVENTION

The method of the present invention allows the computational workload of a seismic process, such as DMO processing to be partitioned unequally and dynamically over multiple processors in a multiprocessor computer to achieve good load balancing.

The invention provides a method for determining how many bins to assign to each processing node of a multiprocessor computer to process a given collection of prestack trace data while achieving good load balancing. The invention also provides a method for efficiently reading different amounts of poststack data from the disk storage system of a multiprocessor computer into different processing nodes of a multiprocessor computer, applying a seismic operator to the data, and then writing the updated poststack data back to the disk storage system.

In the preferred embodiment of the invention, DMO processing is performed on an MPP with a variable number of processing nodes and disks. The preferred configuration of the disk storage system allows a large

contiguous block of data to be transferred between disk and processor node memory in an efficient manner. During a read operation, the data block is partitioned into non-overlapping data subblocks of potentially different sizes, and each data subblock is transferred into a processor node's memory. The first subblock is transferred into the first node's memory, the second subblock is transferred into the second node's memory, and so on. A write operation is the inverse of a read operation. A collection of data subblocks are transferred from node memories, and are effectively concatenated together to form a large contiguous data block. This large data block is then written to the disk storage system. In a read or a write operation the size of any subblock can be zero, which allows any node to be skipped.

In the preferred embodiment of the invention, prestack trace data is read from the disk storage system in successive contiguous blocks to respective node memory in conformance with the most efficient mode of operation of the disk storage system. This data may be read into all or some of the nodes of the MPP. Once this data has been read, the nodes holding the data (so-called "input nodes") determine the number of traces covering each bin in the survey, or preferably of a rectangular bin area. A bin area is composed of one or more contiguous bins in the survey, where the area size is a user-specifiable number of rows and columns. The nodes then broadcast a description of this coverage information to all other nodes in the MPP. Note that since each input node reads in a different set of prestack traces, the coverage descriptions that these input nodes broadcast are not identical.

Each node that will apply the DMO operator (so-called "operator nodes") to prestack data coalesces the information in each broadcast into a single description that reflects the total coverage of survey bins by all input nodes. From this information, the operator nodes determine how to best partition the area of the survey containing covered bins into contiguous blocks of bins, and then how best to partition each block into contiguous subblocks of bins. To achieve good load balancing, each block of bins should be partitioned into subblocks composed of bin areas, such that there are as many subblocks as there are operator nodes, and such that the total trace coverage in each subblock of bins is as close to equal as possible.

In the preferred embodiment of the invention, each block into which the covered bins of the survey are partitioned is composed of a number of horizontally-adjointing bin areas. Each subblock into which these blocks are in turn partitioned is therefore also a number of horizontally-adjointing bin areas.

Thus, operator nodes assigned to an area of the survey in which the coverage is low--for example, an area covered only by far-offset traces--will be assigned more bin areas than operator nodes assigned to an area in which the coverage is high--for example, an area covered by near-offset traces. The smallest assignment containing any bins is a single bin area. The largest assignment is limited only by the amount of memory available on an operator node.

Once the bin area assignments have been determined, the operator nodes load the poststack trace data corresponding to their assigned bins from the poststack data file into their memories. In the preferred embodiment of the invention, the data file containing the poststack traces resides on the disk storage system of the MPP. In order to load this data efficiently, it must be possible to load a single block containing the poststack trace data needed by all of the operator nodes, partition it into contiguous subblocks of potentially varying sizes, and load each

subblock into the appropriate operator node.

This is possible if the data in the file is organized as follows. The survey area is assumed to be a rectangle containing a number of rows and columns of bins. The area is decomposed into a number of smaller areas, each smaller area being the width of the survey but only the height of a previously described bin area. Within each smaller area, the first column precedes the second column, which precedes the third column, and so on for the width of the survey. Within each column, data for the first row precedes data from the second row, which precedes data from the third row, and so on, for the height a bin area. This arrangement makes it possible to read into any node a contiguous block of data formed from any number of contiguous bin areas. It is thus possible to read a contiguous block of bin areas into any number of operator nodes, partitioning the block into contiguous subblocks of zero or more bin areas.

Once the poststack data has been loaded into the memories of the operator nodes, the operator nodes can retrieve the prestack data from the input nodes that hold it, in accordance with the coverage description broadcast from each input node. An operator node only retrieves prestack traces from an input node that holds traces that cover the operator node's assigned bin areas. While some operator nodes have been assigned more bin areas (and hence, more bins) than others, the total number of traces to be processed by each operator node should be as uniform as possible. As a result, each operator node should finish retrieving and processing its prestack traces at about the same time.

When all operator nodes are thus finished, they write their updated poststack trace information back to the poststack trace data file, using an inverse operation to that previously described for reading the poststack trace data. The operator nodes then assign themselves to the next contiguous block of bin areas within the covered bins of the survey. When all such blocks have been processed, the input nodes read in the next block of prestack data, and the previously-described process repeats. When no unprocessed prestack data remains, the DMO computation terminates.

DRAWING DESC:

BRIEF DESCRIPTION OF THE DRAWINGS

FIG. 1 is a block diagram of the abstract massively parallel processor architecture for performing seismic processing in accordance with the methods of the present invention;

FIG. 2 is a block diagram depicting the abstract architecture of a processor node in an MPP used for performing partial or full migration in accordance with the methods of the present invention;

FIG. 3 is a simplified depiction of marine seismic data acquisition;

FIG. 4 illustrates the bin coverage of the "far-offset" trace in the survey depicted by FIG. 3;

FIG. 5 (a-c) illustrate the operation of computing the union of two trace coverage descriptions;

FIG. 6 is a bar graph depicting how the trace coverage for bin areas varies over a large number of columns for marine seismic data;

FIG. 7 is a bar graph depicting how a simple, non-load-balancing

assignment of bin areas to operators for the coverage data of FIG. 6 would result in greatly varying workloads for different operator nodes;

FIG. 8 is a simplified depiction of land seismic data acquisition;

FIG. 9 is a bar graph depicting how the methods of the present invention greatly reduce the variance in workload between different operator nodes for the coverage data of FIG. 6;

FIG. 10 is a bar graph depicting the number of columns assigned to each operator node using the coverage data depicted in FIG. 6;

FIG. 11 depicts an in-memory data structure used for determining per-bin-area trace coverage counts in accordance with the methods of the present invention;

FIG. 12 is a schematic depicting a version of the data structure of FIG. 11 compatible with methods of data transmission over the control and data communications network of the MPP in accordance with the methods of the present invention;

FIG. 13 depicts a data structure showing the organization of a poststack data file in accordance with the methods of the present invention; and

FIG. 14 depicts an example of a survey area for comparison with the data structure of FIG. 13.

DETDSC:

DETAILED DESCRIPTION

In the preferred embodiment of the present invention, methods are provided for supplying prestack input data to processing nodes on a massively parallel processor (MPP) for performing seismic migration, such as a "3D Dip Moveout" or "Kirchhoff" migration.

MPP Overview

FIG. 1 depicts an abstract MPP architecture compatible with the methods of the present invention. The exact details of the data and control communications network are unimportant. In accordance with the methods of the present invention, the communications network 14 need only support the exchange of arbitrary messages between any two processor nodes 16, the ability of any one processor node 16 to broadcast an arbitrary message to all other nodes 16, and the ability of all nodes 16 to synchronize their activities when necessary. Under the preferred embodiment of the invention, the data network 14 should support the transfer of at least 5 megabytes of data per second for each node in the MPP 10. For example, an MPP containing 32 nodes should support at least 160 megabytes/second of aggregate data throughput. FIG. 2 depicts an abstract MPP processing node 16 compatible with the methods of the present invention. Once again, the exact details are unimportant. Under the preferred embodiment of the invention, the node should contain at least 16 megabytes of local random access memory 20 (i.e. "local" memory), and be capable of transmitting and receiving data over the interface 22 to the data communications network 14 at a rate of at least 5 megabytes/second. The CPU 18 can in fact comprise a number of processors.

The preferred embodiment of the invention employs an MPP architecture whose performance scales nearly linearly as the number of nodes 16, amount of local memory 20 on each node, and size of the disk storage

system 12 (i.e. "remote" memory) are increased commensurately. This requires the throughput of the data and control network 14 to scale linearly with the number of processors, since more processors will exchange more data using the network 14. It further requires the throughput of the disk storage system 12 to scale with the number of processors, since more processors will attempt to read more data at the same data rate. By implication, this also requires the capacity of the disk storage system 12 to scale with the number of processors.

A disk storage system architecture that meets this requirement is a disk array, sometimes called a "RAID" architecture, in which a number of usually inexpensive disks are made to appear as a single file system. See, S. J. Lo Verso, M. Isman, A. Nanopoulos, W. Nesheim, E. D. Milne, and R. Wheeler. SFS: A parallel file system for the CM-5. In Proceedings of the 1993 Usenix Conference. Employing a RAID architecture is in itself insufficient to guarantee scalability. The disk storage system must be used in a scalable manner. In general, this requires disk read and write operations to be both synchronized in time and localized over the disk surface, such that each disk is reading or writing from the same place at the same time.

One such MPP that satisfies these requirements is the Connection Machine model CM-5, manufactured by Thinking Machines Corporation of Cambridge, Mass., employing a DataVault or Scalable Disk Array as a disk storage system 12. The I/O system allows any group of nodes 16 to read a block of data from the disk storage system 12, or write a block of data to the disk storage system 12, subject to the constraint that the data block represents a contiguous subset of a file. The block is read into or written from the memories of the group of nodes. The first part of the block is read into or written from the first node in the group; the second part of the block is read into or written from the second node in the group (if there is one). Each succeeding part of the block is read into or written from each succeeding node in the group through the last node in the group.

It should be understood that other multiprocessor computer architectures and other disk storage system architectures that either require or allow a contiguous block of data to be read into or written from a group of nodes 12 of a multiprocessor computer can also be employed by the methods of the present invention.

How Seismic Acquisition Techniques can Create Load Imbalance FIG. 3 shows a simplified 3D marine seismic data acquisition scenario. In actual contemporary practice, a seismic acquisition vessel might tow two streamers 32, which can be up to 5 kilometers in length. Typically a source or airgun array 34 operates in conjunction with a streamer 32 having up to 240 receivers 36 (hydrophones). In addition, survey vessels 30 often operate in pairs, one vessel 30 firing seismic sources 34, and both vessels recording the resulting echoes at the receivers 34. The area over which the seismic survey is conducted is partitioned into bins, as shown in FIG. 3. Each trace recorded during a survey crosses a number of bins 38. During migration, a prestack trace is processed by application of a mathematical operator once for every bin 38 under the trace's "coverage," and superimposed with other traces processed into the same bin. For example, the coverage of a trace in a 3D Dip Moveout program is a line 40 between the seismic source 34 and trailing receiver 36, as depicted in FIG. 4. Thus, in the present application the term "coverage" means an identification of the bins containing seismic data associated with a particular trace. In practice, such a "far offset" trace may cross 400 such bins 38, and an average trace may cross 240 bins. Marine prestack data is usually collected into "common shot gathers" consisting of the traces collected from each receiver on the streamer from a single

shot.

FIG. 5 shows how the coverage from the far-offset traces of two common shot gathers from shots taken in succession combine to create workload imbalance. The first shot coverage 50 (FIG. 5a) combines with the second shot coverage 52 (FIG. 5b) to form the combined coverage 54 (FIG. 5c). In the combined coverage 54, the darker crosshatching 56 depicts those bins that are covered by the far-offset traces of both shots. Because the amount of work to be done when processing a bin depends on the number of traces whose coverage includes the bin, processors assigned to bins with two-trace coverage will have more work to perform than those assigned to bins with single-trace coverage. When more than two shots at a time are considered, and when the streamers contain the typical number of receivers used in actual marine seismic acquisition, and when all of the traces recorded from each streamer are considered, the load imbalance problem can be significant, with some bins covered by more than a few thousand times as many traces as others. FIG. 6 shows the trace coverage of a line of 95 bin areas, each bin area consisting of 4 columns of bins and 8 rows of bins (e.g. 32 bins), using data from an actual marine seismic survey. The streamer contained 144 receivers with a maximum offset (distance from source to receiver) of just over 3 km. The coverage data was generated from 32 common shot gathers. The peak coverage value is 3092 traces in a single bin area, whereas the smallest non-zero value is 2 traces in a single bin area. FIG. 7 shows how many traces each processor of a 24-processor MPP would process if the bin areas of FIG. 6 were assigned respectively to the processors, such that each processor was assigned 4 bin areas (i.e., rectangular areas consisting of 16 columns and 8 rows or 128 bins), except for the last processor, which would be assigned 3 bin areas. The busiest processor would process almost 12,000 traces, whereas the least busy processor would process only 5 traces. The foregoing discussion considered only marine seismic data acquisition. However, load balancing problems are introduced in land seismic data acquisition as well. In land seismic acquisition, multiple parallel lines of receivers receive reflections from shots, which are located along multiple perpendicular parallel lines 101,103 as shown in FIG. 8. The lines form a grid. FIG. 8 depicts an ideal 3D land survey geometry. The shot points 100 are located along horizontal lines 101 and are indicated with X's. The receiver points 102 are located along vertical lines 103 and are indicated with filled circles.

Land prestack data is usually collected into "common receiver gathers" consisting of the traces collected from a single receiver from all of the shots. Since in general a ****common** **receiver** **gather**** consists of data from shot points located in all directions around, and at various distances from the receiver location, the trace coverage of such a gather tends to be greater in bins nearer the receiver location than those farther from it. Thus, when multiple gathers are combined, there will be bins with substantially higher trace coverage than others if the locations of the receivers in the collection of gathers are close together.

The methods of load balancing of the present invention are capable of handling both marine and land acquisition geometries.
Determining Trace Coverage for Load Balancing

In accordance with the methods of the present invention, MPP nodes are designated as input or operator nodes, and the input nodes load a collection of prestack traces. Once this prestack trace data has been read, the input nodes determine the number of traces covering each rectangular bin area. FIG. 11 depicts a coverage map 110 of a data structure compatible with the methods of the present invention in which

the input nodes can store coverage information. The preferred means for filling this data structure is as follows:

1. For each trace i each input node has loaded, the node determines the smallest rectangular bounding box, $B_{sub.i}$, in a Cartesian of the trace. If the migration application is a DMO computation, the coverage is a line drawn between the shot and receiver locations for that trace (see FIG. 4). The shot and receiver location is found in a header section that precedes the data portion of the trace.
2. Each input node unions together each such bounding box $B_{sub.i}$ to create the smallest bounding box, $B_{sub.L}$, that encloses the individual trace bounding boxes.
3. Each input node broadcasts to all other nodes (input and operator nodes) in the MPP a compact description of its bounding box $B_{sub.L}$ created in step 2. In the preferred embodiment of the present invention, this broadcast consists of the leftmost and rightmost x coordinates of the box, and the topmost and bottommost y coordinates of the box.

Each node that receives such a broadcast unions the described bounding box $B_{sub.L}$ with a global bounding box description, $B_{sub.G}$, such that after all broadcasts have received, $B_{sub.G}$ describes the smallest bounding box that encloses each node's $B_{sub.L}$.

4. All nodes now have enough information to create a coverage map 110, such as depicted in FIG. 11, to hold trace coverage information for all of the data each input node has loaded. This coverage map is referred to as the "coalesced map."

The base row field 111 of the data structure contains the lower left y coordinate of $B_{sub.G}$ divided by the height of a bin in the survey, and then rounded down to the next smallest multiple of the bin area height (the number of rows of bins that are grouped together to form a bin area).

The base column field 112 of the data structure contains the lower left x coordinate of $B_{sub.G}$ divided by the width of a bin in the survey, and then rounded down to the next smallest multiple of the bin area width (the number of columns of bins that are grouped together to form a bin area).

The area width field 113 contains the number of columns of bins that are grouped together to form a bin area. This information may also be encoded in the DMO computation as a constant number, in which case it need not be included in the trace coverage data structure.

The area height field 114 contains the bin area height. This information may also be encoded in the DMO computation as a constant number, in which case it need not be included in the trace coverage data structure.

The number of area rows field 115 contains the bin area width. This information is computed from the height of the bounding box $B_{sub.G}$, rounded up to the next higher multiple of the bin area height.

The number of area columns field 116 contains the number of columns of bin areas that are described by the data structure. This information is computed from the width of the bounding box $B_{sub.G}$, rounded up to the next higher multiple of the bin area width.

The pointer to coverage counts field 117 contains a pointer to a 2-dimensional array 118 (FIG. 11) in which the trace coverage counts for individual bin areas will be stored. This array can be allocated once the number of area rows and number of area columns is known, since these two

pieces of information determine the height and width of the array. When the array is allocated, it is initialized to contain 0 in each element. The bin area enclosing the base row 111 and base column 112 of the coverage map 110 is the array element 119.

It should be understood that other data structures that allow essentially the same information to be stored are within the scope of the methods of the present invention.

5. Input nodes create a coverage map 110 into which they place trace coverage information for each bin area covered by the union of

For each loaded trace, the input node determines which bin areas are crossed by the trace. For each such bin area, the node increments by one the corresponding element in the trace coverage counts array 118 of the coverage map 110.

At this point, each input node possesses a coverage map that describes how each trace it has loaded covers the seismic survey. Each node then sends the information in its coverage map to all other nodes in the MPP. Under the preferred embodiment of the invention, this information is sent as follows:

1. Each input node sends two broadcasts. The first broadcast contains the length of the second broadcast. This length is sufficient to include both the fixed size portion of the coverage map and the variable size portion of the coverage map (i.e., the coverage count array). The second broadcast contains the coverage map, rendered in a form that can be sent through the control and data network 14 of the MPP 10 and restored into a machine readable form within each processor node 16. FIG. 12 depicts a broadcast format compatible with the methods of the present invention.
2. When a node receives the first broadcast, it allocates a buffer capable of holding the second broadcast. After the node receives the second broadcast into the buffer, it processes the data in the buffer to recreate a copy of the coverage map data structure 110 sent by the broadcasting node.
3. Each node then adds the information in the received coverage map to its coalesced coverage map. This is done by adding element-by-element the coverage count information in the received coverage map to the coverage count information in the coalesced coverage map.

Bin Allocation for Load Balancing

After each input node has sent its coverage map information, all nodes possess identical coalesced coverage maps that describe trace coverage information for each covered bin area in the survey. From this information, all nodes determine in parallel how to best allocate bin areas to operator nodes subject to optimal load balancing. Each allocation computation is the same and the computation of one node is independent of the computation on other nodes. However, since the data the nodes begin with is identical, and since the allocation computation is identical, each node determines the same allocation of bin areas to operator nodes. Thus, when all nodes have finished the allocation computation, each possesses the same information about bin area allocation.

Many allocation algorithms are possible in accordance with the methods of present invention. The preferred method is as follows:

1. For the first swath of rows that contains covered bin areas, the average bin area coverage value is computed. This is done by summing the coverage counts for each bin area column and dividing by the number of bin areas containing coverage values greater than zero.
2. An initial target coverage value to be assigned to each operator is

determined. This target value is simply the average coverage value just computed multiplied by half the maximum number of bin areas each operator node is able to process at any one time.

3. The first operator node is assigned enough bin areas to just exceed the target value. The first bin area assigned is the leftmost bin area in the swath containing covered bins that has yet to be processed. No more bin areas are assigned to the operator node than a previously-specified maximum number of bin areas, and no bin area beyond the rightmost bin area in the swath containing covered bins is assigned.
4. Remaining operator nodes are assigned bin areas as in step 3, except the first bin area assigned is the one to the right of the last bin area assigned to the previous operator node.

FIG. 9 shows how the resulting allocation of bin areas to operator nodes evens out the number of traces to be processed by each operator node, for the coverage data shown in FIG. 6. As compared to FIG. 7, the variance in the number of traces assigned to each node is significantly smaller, as is the maximum number of traces assigned to any single node. FIG. 10 shows how the allocation algorithm assigns a different number of columns to different nodes to achieve this improved load balancing. In this case, the bin area width was 4 columns; thus, each node is assigned a multiple of four columns. The nodes assigned the most columns were assigned 44 columns (11 bin areas), whereas the nodes assigned the least columns were assigned 8 (2 bin areas).

Poststack Data Transfer

Once the bin area assignments have been determined, the operator nodes load the poststack trace data corresponding to their assigned bins from the poststack data file into their memories. In the preferred embodiment of the invention, the data file containing the poststack traces resides on the disk storage system or remote memory 12 of the MPP 10. As has been noted, it must be possible to load this data in a single operation. FIG. 13 depicts a poststack data file organization consistent with the methods of this invention that allows a different number of columns of poststack data to be loaded into different operator nodes in a single input operation from the disk storage system 12. FIG. 14 illustrates an example of a survey area 160 for better understanding the data file organization of FIG. 13.

The survey area 160 covered by the poststack data file 130 is assumed to be a rectangle containing a number of rows and columns of bins 166. The survey area 160 is decomposed into a number of swaths 162, each swath area being the width W of the survey area 160 but only the height H of a bin area. A bin area is one or more contiguous bins, preferably a rectangle, such as denoted by 164 in FIG. 14. Within each swath 162, the first column precedes the second column, which precedes the third column, and so on for the width of the swath. Within each column, data for the first row precedes data from the second row, which precedes data from the third row, and so on, for the height of a bin area.

Thus, in FIG. 13, the poststack data file 130 is composed of a sequence of blocks, each B bytes long. Each block contains the poststack data for a single bin. This data may comprise 1 or more traces. The first block 131 contains poststack data for the bin at column 0 row 0, the bin in the upper left corner of the area covered by the stack file. The second block 132 contains data for the bin at column 0 row 1. Succeeding blocks in the poststack data file 130 contain data for rows 2 through $H-1$ in column 0, where H is the height of a bin area. The block 141 contains data for column 0 row $H-1$. The block 142 immediately following block 141 contains data for column 1 row 0. Block 151 contains data for column $W-1$ row $H-1$.

Block 152, which immediately follows block 15 1 contains data for column 0 row H.

The poststack data file arrangement depicted in FIG. 13 thus allows a group of data blocks comprising any number of columns, starting at any initial column, to be transferred between the local memories 20 of the processor nodes 18 and the poststack data file 130 on the disk storage system 12 in a single large data block in a single input or output operation. The number of rows in a data group transferred into or out of each node 18 must be equal to the height of a bin area, and the first row in a data group to be transferred must be a multiple of the bin area height. The number of columns in a data group to be transferred into or out of each node 18 can be different. While the preferred embodiment contemplates having a fixed number of rows in each data group, an alternative could fix the number of columns and vary the number of rows. Each node transfers $c*B*H$ bytes from the large data block to transfer c columns, where c is the number of bin areas allocated to the node 18 multiplied by the number of columns in a bin area.

Once the poststack data has been loaded into the memories of the operator nodes, the operator nodes can retrieve the prestack data from the input nodes that hold it, and apply the DMO operator to the prestack data to update the poststack data. When all operator nodes are finished processing prestack data that covers their bin assignments, they write their updated poststack trace information back to the poststack trace data file, using an inverse operation to that previously described for reading the poststack trace data.

CLAIMS:

I claim:

1. A method of assigning prestack seismic input data of a seismic survey comprising an array of bins to processing nodes of a multiprocessor computer having remote and local memory comprising the steps of:

- a) dividing the processing nodes into a plurality of input and operator nodes;
- b) reading prestack seismic input data from remote memory into the local memory of input nodes;
- c) determining the coverage of prestack seismic input data associated with each bin in the seismic survey;
- d) broadcasting the coverage to at least the operator processing nodes; and
- e) assigning bins to operator processing nodes based on the coverage in each bin, the amount of coverage assigned to each processing node being generally equal.

2. The method of claim 1, where for a number of operator nodes including the steps of:

- f) each operator node reading poststack seismic data for its assigned bins from remote memory to its local memory;
- g) each operator node reading into its local memory its assigned coverage of prestack data from input node local memory;
- h) each operator node applying a dip moveout migration operation to its prestack coverage and updating its poststack data; and
- i) each operator node writing its updated poststack data from local memory to remote memory.

3. The method of claim 1, in said dividing step a), some of said nodes being operable as both an input and operator node.

4. The method of claim 1, said reading step b) comprising the substeps of partitioning the prestack seismic input data into contiguous, non-overlapping data blocks and transferring successive data blocks to the local memory of successive input nodes.

5. The method of claim 1, in said determining step c) the prestack seismic input data comprising trace data, for each input node the steps of
determining the smallest individual rectangular bounding box enclosing the bins for each trace coverage the input node has loaded, and
unioning all bounding boxes to create the smallest unioned bounding box enclosing all individual bounding boxes.

6. The method of claim 1, said broadcasting step d) comprising the substeps of each input node sending--a first message indicative of the size of the coverage and a second message indicative of coverage contained within its local memory.

7. The method of claim 1, said assigning step e) comprising the substeps of:
dividing the seismic survey into contiguous blocks of bins,
partitioning each block into a plurality of subblocks with the number of subblocks equal to the number of operator nodes and the trace coverage in each subblock approximately equal.

8. A method of transferring poststack seismic data of a seismic survey area between remote memory and a plurality of local memories of a multiprocessor computer, where the seismic survey area comprising two-dimensions, columns and rows, of bins comprising the steps of:
dividing the seismic survey area into bin areas comprising one or more contiguous bins of seismic data;
arranging a data file of the poststack seismic data in remote memory as a sequence of data blocks where each block contains the data in a single bin and the sequential order of the blocks correspond to contiguity of the respective bins in one dimension;
coalescing sequential data blocks into data groups, where the corresponding bin groups have one dimension fixed and the other dimension variable, and
transferring in a single operation the data file between remote memory and local memories where a first data group is transferred between remote memory and a first local memory and a second data group is transferred between remote memory and a second local memory.

9. The method of claim 8, where the one dimension fixed is the number of rows and the other dimension variable is the number of columns.

10. The method of claim 9, the number of rows being equal to the height of the bin area.

11. The method of claim 8, the seismic survey area comprising a rectangular array of bins which is a subset of a larger seismic survey.

12. The method of claim 8, the transferring step comprising a first transfer substep where the data file is read from remote memory into the local memories associated with operator processing nodes, and
a second transfer substep where the data file is written from the local memories into the remote memory.

13. The method of claim 12, including the steps of the operator nodes:
retrieving prestack data from a plurality of input processing nodes;
applying a DMO operator to the prestack data;

updating the data file in each local memory prior to writing the data
file to remote memory.

=> logoff

ALL L# QUERIES AND ANSWER SETS ARE DELETED AT LOGOFF
LOGOFF? (Y)/N/HOLD:n

2- (TULSA)
AN - 527840
Title → TI - EXPERIMENTAL STUDY OF AN ADVANCED THREE-COMPONENT BOREHOLE SEISMIC
Author → AU - SLEEFE, G E; ENGLER, B P
OS - SANDIA NATIONAL LABS
Organizational Source SO - SANDIA NAT LAB REP NO SAND-91-1265C (DE91014652) (1991) (1 MICROFICHE
WITH 5 PP; 5 REFS)
LA - ENGLISH
DT - (GR) GOVERNMENT REPORT
IT - *THREE COMPONENT GEOPHONE; *CROSSHOLE METHOD; *EXPLORATION; *GEOPHONE;
*GEOPHYSICAL EQUIPMENT; *GEOPHYSICAL EXPLORATION; *PROCEDURE;
*PROFILING;
*RECORDING; *SEISMIC EQUIPMENT; *SEISMIC EXPLORATION; *SEISMIC
RECORDING;
*SEISMIC REFLECTION METHOD; *THREE COMPONENT RECORDING; *VERTICAL
SEISMIC
PROFILING; ACCELEROMETER; BOREHOLE; CASINGS; CHART; CONNECTOR; COUPLING
(MECHANICAL); DATA; DATA ACQUISITION; DEEP HOLE GEOPHONE; FINITE
ELEMENT;
FITTING; FREQUENCY; GEOPHYSICAL DATA; GRAPH; HARRIS CO, TEX; HUMBLE OIL
FIELD; INSTRUMENT; MATHEMATICS; NOISE; NORTH AMERICA; PHOTOGRAPH;
PIEZOELECTRIC GEOPHONE; PRESSURE; REFLECTION (SEISMIC); SEISMIC DATA;
SEISMIC NOISE; SEISMIC WAVE PROPAGATION; SIGNAL TO NOISE RATIO; SONDE;
SUBSURFACE PRESSURE; SUBSURFACE TEMPERATURE; TEMPERATURE; TEXAS;
TRANSMISSION (SEISMIC); UNITED STATES; WAVE FREQUENCY; WAVE PHENOMENON;
WAVE PROPAGATION; WESTERN US
MH - *THREE COMPONENT GEOPHONE
CC - GEOPHYSICS
AB - AN ADVANCED 3-COMPONENT BOREHOLE SEISMIC RECEIVER HAS BEEN DESIGNED,
DEVELOPED AND TESTED. THIS RECEIVER WAS DESIGNED WITH THE AID OF FINITE
ELEMENT VIBRATION MODELING TO BE FREE OF SIGNIFICANT CLAMP RESONANCES
BELOW 2,000 HZ. THIS BROAD FREQUENCY RANGE MAKES THIS SONDE WELL SUITED
FOR CROSS-WELL SEISMIC IMAGING APPLICATIONS. STATE-OF-THE-ART
PIEZOELECTRIC ACCELEROMETERS ARE USED AS THE 3-COMPONENT SENSORS AND
PROVIDE SIGNAL ENHANCEMENT RELATIVE TO CONVENTIONAL GEOPHONES. THE USE
OF THESE ACCELEROMETERS OFFER A SIGNAL-TO-NOISE ENHANCEMENT OF APPROX.
20 DB AT 1,000 HZ OVER MOVING-COIL SEISMIC GEOPHONES. A PROTOTYPE
ACCELEROMETER-BASED SONDE WAS FIELD TESTED AT THE TEXACO HUMBLE FIELD TO
DETERMINE ITS PERFORMANCE CHARACTERISTICS. THE ADVANCED SONDE EXHIBITED
SIGNIFICANTLY IMPROVED COUPLING RELATIVE TO THE VSP (VERTICAL SEISMIC
PROFILE) TOOL AS EVIDENCED BY INCREASED BANDWIDTH AND SIGNAL-TO- NOISE
RATIO. ADDITIONALLY, THE ADVANCED SONDE PRODUCED SIGNALS WHICH RIVAL
THOSE PRODUCED BY THE BURIED/CEMENTED GEOPHONES.
PY - 91



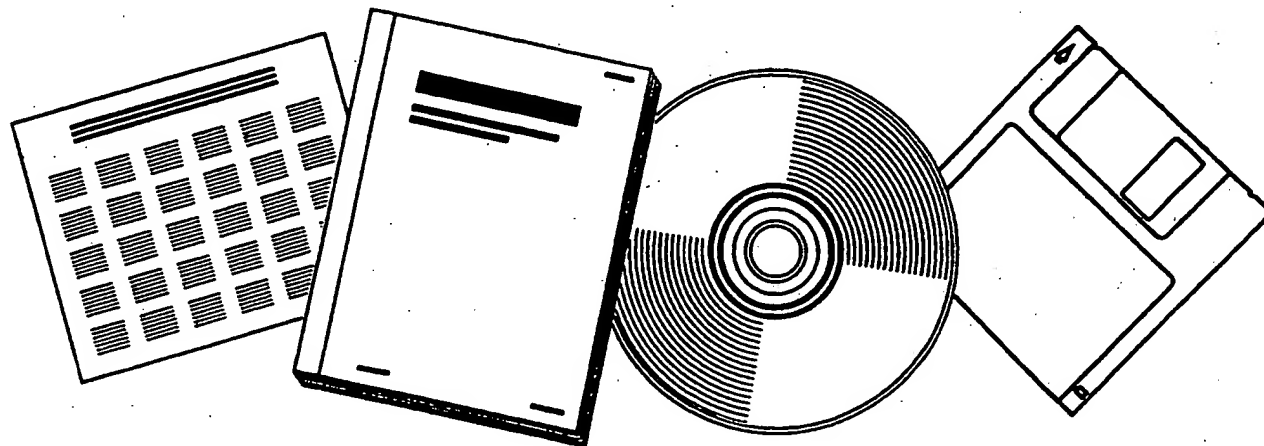
DE91014652

NTIS[®]
Information is our business.

EXPERIMENTAL STUDY OF AN ADVANCED THREE-COMPONENT BOREHOLE SEISMIC RECEIVER

SANDIA NATIONAL LABS.
ALBUQUERQUE, NM

1991



U.S. DEPARTMENT OF COMMERCE
National Technical Information Service

*Bookmark
this site today!*

The Department of Commerce Online International Trade Center Bookstore

Managed by the National Technical Information Service

The Department of Commerce International Trade Center Bookstore brings together a world-class collection of publications from government and non-profit organizations. This collection is now available through a new online bookstore.

Tap into information from these leading research institutions:

- The Brookings Institution
- Center for Strategic and International Studies
- Export-Import Bank of the United States
- Library of Congress
- World Bank
- United Nations
- Organization for Economic Cooperation and Development
- Battelle

New features and collections added regularly!

Visit the web site at
<http://tradecenter.ntis.gov/>

An essential online tool providing one-stop access to the very best international trade information available anywhere.

SEARCH & ORDER ONLINE FROM THIS GROWING COLLECTION:

Search the complete ITC Bookstore by keyword or narrow your search to a specific collection.

A WIDE RANGE OF SUBJECTS:

International trade related subjects in the Bookstore include agriculture and food, behavior and society, business and economics, communication, computers, energy, environmental pollution and control, health care, military sciences, and transportation.

BROWSE BY REGION: Review titles that focus on issues as they relate to seven world regions. Narrow your focus by combining this feature with keyword searching.

BROWSE BY INDUSTRY SECTORS:

Select from more than 20 industry sectors and their sub-sectors. Combine this feature with a keyword search for a more precise list of titles.

EASY ACCESS TO OTHER TRADE RELATED INFORMATION:

Use the site to easily locate other trade related sites, to find international trade bestsellers, and to search for industry standards.



U.S. DEPARTMENT OF COMMERCE
Technology Administration
National Technical Information Service
Springfield, VA 22161 (703) 605-6000

Experimental Study of an Advanced Three-Component Borehole Seismic Receiver
G. E. Sleepe, and B. P. Engler, Sandia National Laboratories*

SUMMARY

An advanced three-component borehole seismic receiver has been designed, developed, and tested. This receiver was designed with the aid of finite element vibration modeling to be free of significant clamp resonances below 2000 Hz. This broad frequency range makes this sonde well suited for cross-well seismic imaging applications. State-of-the-art piezoelectric accelerometers are used as the three-component sensors and provide signal enhancement relative to conventional geophones. The use of these accelerometers offer a signal-to-noise enhancement of approximately 20 dB at 1000 Hz over moving-coil seismic geophones. Additional features of the sonde include high temperature/pressure operation, small size, lightweight, field-durable construction, and multi-station expansion capability. A prototype accelerometer-based sonde was field tested at the Texaco Humble Field to determine its performance characteristics. A borehole explosive source was used to test the sonde in a cross-well configuration (815 ft well-to-well separation). For comparison purposes, similar cross-well tests were performed using a commercial VSP-type tool and buried/cemented geophones. The advanced sonde exhibited significantly improved coupling relative to the VSP tool as evidenced by increased bandwidth and signal-to-noise ratio. Additionally, the advanced sonde produced signals which rival those produced by the buried/cemented geophones.

INTRODUCTION

The bandwidth associated with conventional surface-seismic and VSP techniques for imaging deep petroleum reservoirs (Coffeen, 1986) is typically less than 150 Hz. With the advent of cross-well seismic techniques, the bandwidth is potentially increased well beyond 150 Hz due to the shorter propagation paths and the improved seismic coupling at depth. As a result, there is now a need for both borehole seismic sources and receivers that have bandwidths on the order of 1000 Hz to take advantage of the high resolution capabilities of cross-well imaging (Bloch, 1990). It has long been recognized (Galperin, 1985), however, that conventional VSP wall-locked sondes exhibit structural resonances in the 150 Hz to 400 Hz range. The presence of such tool resonances results in significant distortion of the seismic signals recorded during high-resolution cross-well surveys. Therefore, it is desirable to develop a wall-locked three-component sonde that is free of resonances at least below 1000 Hz. Even with a resonant-free tool, however, new three-component sensors need to be investigated for this broad-band application. While conventional geophones are clearly the appropriate sensor for low-frequency applications (Stanley, 1986), their performance degrades at the cross-well seismic frequencies. Therefore, the optimal sensor for cross-well seismic sondes needs to be determined. A further limitation of conventional VSP-type tools is that they do not readily allow expansion to multi-station configurations. The ability to simultaneously clamp multiple sondes in a borehole is essential to the commercial success of three-component cross-well surveys.

Considering the limitations of existing borehole seismic sondes, a program was undertaken to develop a borehole seismic receiver with the following performance characteristics: no resonances below 1000 Hz and preferably no significant resonances below 2000 Hz; accommodates advanced seismic sensor technology that offers signal enhancement at the cross-well seismic frequencies; provides for multi-station inter-connection; and withstands the oil-well environment including elevated temperatures/pressures and rough handling. A prototype seismic sonde with these characteristics has been developed and tested. In this paper, we describe the features of this sonde and present cross-well seismic data obtained from the advanced sonde. The performance of the sonde will be illustrated by comparisons with field data from a commercial VSP-type tool and buried/cemented geophones.

SONDE DESCRIPTION AND DESIGN

The present configuration of the Advanced Borehole Receiver (patent pending) consists of two pressure housings terminated with standard Gearhart-Owens seven conductor cable connectors, one on either end of a clamping assembly section. One housing contains the triaxially arranged accelerometers and the other the electric gearmotor. This gearmotor drives a rectangular piston perpendicular to the tool using a right angle translation unit to clamp the tool into the borehole. Since the right angle translation unit resides outside of the pressure housings, a high temperature and pressure rotary seal is used to insure integrity where the drive shaft breaches the gearmotor bulkhead. A photograph of the prototype Advanced Borehole Receiver is shown in Figure 1.

The primary design criteria for the Advanced Borehole Receiver are given in Table 1. The philosophy used to obtain these criteria required breaking the design into problem areas that could be solved individually. The identified design problem areas were: 1) temperature and pressure, 2) minimal overall length and maximum outside diameter of 4 inches, and 3) frequency response of the tool. Initial design solutions which satisfied the environmental and size constraints were then studied using finite element analysis to determine the clamped-tool frequency response. The design process then involved various iterations until a final design prototype which met the specifications of Table 1 resulted.

The temperature and pressure criteria were met initially by using type 17-4 stainless steel with a quarter inch wall thickness for the pressure housings. High temperature and high pressure O-rings were used as seals at the critical surfaces. Also, a high temperature and pressure rotary seal was used at the bulkhead / drive-shaft interface. A standard right angle drive device was slightly modified to withstand the pressure and a directly replaceable version that will handle both the temperature and pressure is available. A high temperature electric motor with variable gear trains was selected as the drive mechanism. Since the motor resides inside a pressure housing, its pressure specifications are lower

DISCLAIMER

This report was prepared as an account of work sponsored by an agency of the United States Government. Neither the United States Government nor any agency thereof, nor any of their employees, makes any warranty, express or implied, or assumes any legal liability or responsibility for the accuracy, completeness, or usefulness of any information, apparatus, product, or process disclosed, or represents that its use would not infringe privately owned rights. Reference herein to any specific commercial product, process, or service by trade name, trademark, manufacturer, or otherwise does not necessarily constitute or imply its endorsement, recommendation, or favoring by the United States Government or any agency thereof. The views and opinions of authors expressed herein do not necessarily state or reflect those of the United States Government or any agency thereof.

The size and weight design constraints led to two possible clamp-arm mechanisms: an angular-type clamp-arm, as per conventional VSP tools; and the clamping piston concept. Angular-type clamp arms were then ruled out since initial finite element modeling indicated significant clamp-arm resonances below 1000 Hz. Various clamping piston arrangements were then investigated to meet the environmental, physical, and frequency response constraints. The resulting design is a rectangular clamping piston that is driven by an electric gear-motor perpendicular to the tool axis. The clamping piston allows for 1.5 inches of travel, and accommodates adapters to allow clamping in boreholes ranging from 4.25 in. o.d. to 9 in. o.d. For prototype testing, a standard Gearhart-Owens seven conductor cable head was adapted to the ends of the pressure housings.

In order to evaluate the frequency response of the design, finite element analysis using NASTRAN code was performed on a model of the design. This entailed creating a representative mesh of the entire tool and establishing anchor or pin points about which the tool could move or flex. Different test cases were run in which the number and location of the pin points were varied to determine if any tool resonances existed. The results of these tests indicated where modifications needed to be made to remain within the design goal. This process was repeated until the results indicated the potential for a flat tool response out to 2.0 kHz.

An important issue for this advanced seismic receiver was the selection of appropriate three-component sensors. Both theoretical and experimental investigations were undertaken to determine the optimal sensor for cross-well applications. As a result of these studies, we developed the required specifications for a signal-enhancing cross-well seismic accelerometer. These low-noise accelerometers were then custom manufactured by Wilcoxon Research, Gaithersburg, Md. It was found that the use of these low-noise piezo-electric accelerometers offer some significant advantages over conventional geophones. In particular, these accelerometers do not exhibit the 'spurious resonance' problem common to geophones (Stanley, 1986). Additionally, accelerometers are insensitive to their mounting orientation and therefore do not require the gimbal mounts often utilized in geophone-based sondes. Another difference, and perhaps most important, is that these custom-designed low-noise piezo-electric accelerometers are more sensitive than geophones at the cross-well seismic frequencies. This results since the electronic noise of the custom accelerometer is lower than the electronic noise of the best geophones at frequencies above approximately 150 Hz. To illustrate this point, Figure 2 displays seismic noise data measured with the accelerometers in two oil wells. The higher noise level in Well C30 results from nearby active oil-well pump-jacks. Also indicated in Figure 2 is the theoretical noise limit for moving-coil seismic geophones and the noise specification for the present low-noise accelerometers. It is apparent from Figure 2 that the accelerometers can offer as much as a 20 dB improvement in signal detection (and hence signal-to-noise ratio) at 1000 Hz.

A prototype sonde which meets the specifications of Table 1 was manufactured by OYO Geospace, Houston, TX. This prototype underwent significant laboratory testing to verify the clamping force, pressure integrity, frequency response, and compatibility with accelerometers. These laboratory tests served as a quality assurance measure prior to deploying the prototype in an oil-field environment.

Table 1

Advanced Borehole Seismic Receiver Specifications

Dimensions:	16" length by 4" o.d.
Weight:	30 lbs
Clamp force-to-weight ratio:	at least 5:1
Working Pressure:	10,000 psi
Working Temperature:	200° c (mechanical) 125° c (with current accelerometers)
Exposed Material:	Stainless Steel
Operates On:	7-conductor wireline (G.O.) or Multistation interconnect
First Computed Resonance:	2.1 kHz

CROSS-WELL SEISMIC DATA

During March of 1991, the advanced borehole seismic receiver prototype underwent a substantial set of field trials. The tests were held at the Texaco Humble Field Site near Houston, Tx. This site is an active oil-producing field with several wells available for cross-well seismic testing. At the site, both cross-well and VSP data were collected using the accelerometer-based sonde. Figure 3 is a representative data set obtained from the advanced sonde in the cross-well configuration. Figure 3 is a common-receiver gather (receiver depth of 1200 ft.) obtained in a cross-well configuration of 815 ft well-to-well spacing. The seismic source was a 10 gram explosive p-wave source (Chen et al., 1990) which generates wide-bandwidth signals. Figure 4 illustrates a common receiver gather for the same exact shots as used for Figure 3, but recorded by nearby cemented and buried geophones. The offset of the buried geophones from the source well was 1015 ft. In Figure 5, a commercial VSP-type tool was used to form a common receiver gather using the same parameters as Figure 3, i.e., 815 ft well-to-well spacing, with receiver clamped at 1200 ft depth.

Comparing Figures 3 and 4, it is clear that the basic character of the seismic sections is the same for both the buried geophones and the accelerometer-based sonde. In other words, the Advanced Borehole Receiver appears to couple adequately to the casing and is free from significant resonances in the pass-band (10 Hz to 1400 Hz). On the other hand, the commercial VSP tool, as indicated in Figure 5, produces "ringy" first arrivals indicative of resonances in the pass-band. Thus the advanced sonde provides for better coupling than the VSP tool at the cross-well seismic frequencies.

In order to quantify the signal-enhancement characteristics of the accelerometer-based sonde, spectral analysis of the p-wave arrivals from Figures 3, 4 and 5 was performed. Both average p-wave spectra and average noise spectra were computed for each section, thereby allowing a determination of the signal-to-noise ratio versus frequency. Figure 6 displays the results from this spectral analysis and clearly indicates the increased bandwidth and signal-to-noise

enhancement of the accelerometer-based sonde. Specifically, note that the accelerometers offer an approximately 25 dB signal-to-noise enhancement at 1000 Hz relative to the buried geophones.

CONCLUSIONS

A prototype accelerometer-based seismic receiver has been designed, developed and tested. Cross-well seismic testing of the receiver indicates excellent coupling of the tool to the borehole to frequencies of at least 1400 Hz. The signals generated by the advanced sonde are considerably higher in resolution than those produced by a VSP-type tool. The receiver also appears to offer signal enhancement relative to buried and cemented geophones. This high resolution receiver should prove useful in improving the effectiveness of cross-well seismic surveys.

ACKNOWLEDGEMENTS

This program is funded by the U.S. Department of Energy under contract DE-AC04-76DP00789 and conducted under the auspices of DOE's Oil Recovery Technology Partnership. We greatly acknowledge the joint government/industry cost-shared participation of OYO Geospace, Houston Texas, (for developing and manufacturing the prototype sonde), Exxon Production Research Company (for participating in the field experiments and operating their borehole seismic source), and Texaco E. & P. Technology Division (for providing the Humble site and its field equipment). We also wish to greatly acknowledge the efforts of P.M. Drozda, Sandia National Laboratories, for his assistance in field testing the prototype.

REFERENCES

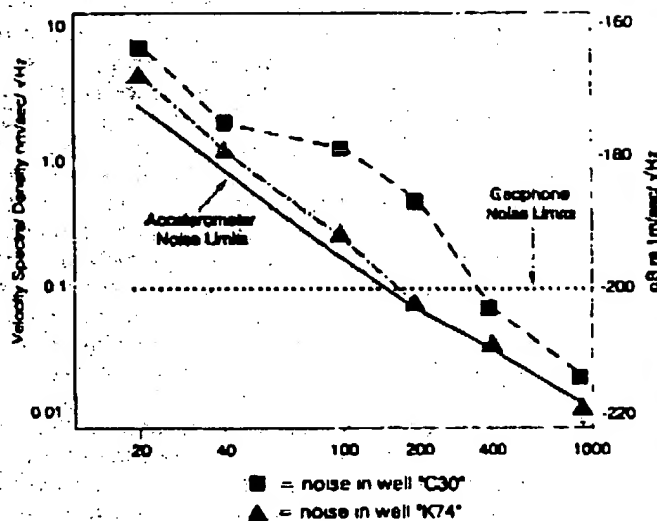
- Colfeen, J.A., 1986, Seismic exploration fundamentals, Second Edition, Penwell Publishing, Tulsa, Ok.
- Bloch, M., 1990, Borehole Seismic Techniques: Review and Outlook, Institut Francais Du Petrole, Report No. 37915.
- Galperin, E I, 1985, Vertical seismic profiling and its exploration potential, D. Reidel Publ. Co., Boston, MA. pp 25-26.
- Stanley, P.J., 1986, The geophone and front-end fidelity, First Break, Vol. 4, No. 12, pp. 11-14.
- Chen, S.T., Zimmerman, L.J., and Tugnait, J.K., 1990, Subsurface imaging using reversed vertical seismic profiling and crosshole tomographic methods, Geophysics, Vol. 55, No. 11, pp. 1478-1487.

Figure 1



Photograph of prototype
Advanced Borehole Receiver

Figure 2



Seismic noise measured in wells at Texaco Humble Site. Measured using low-noise accelerometers clamped at 1200 ft depth.

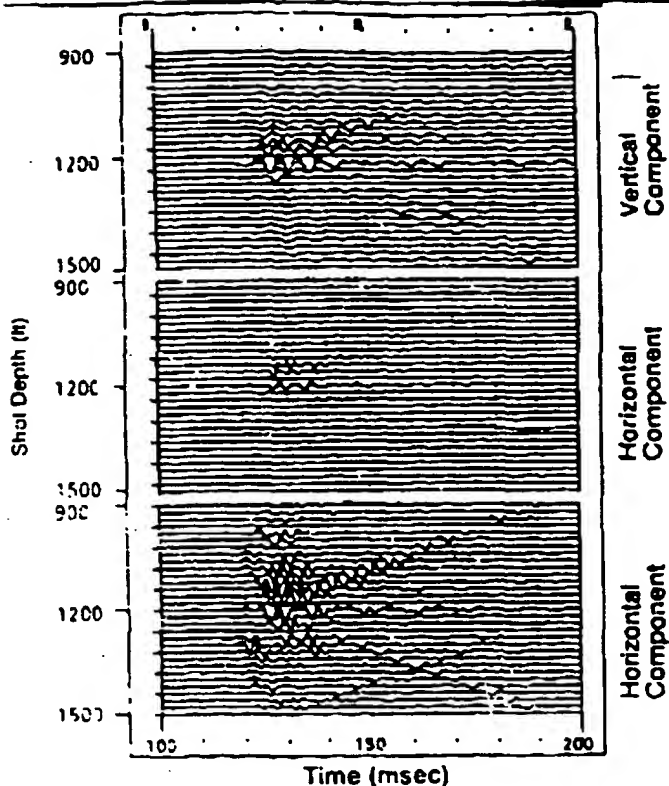


Figure 3. Common-receiver gather obtained from Advanced Borehole Receiver (Accelerometer-Based). Receiver depth is 1200 ft, well-to-well spacing is 815 ft, and fixed display gain is used.

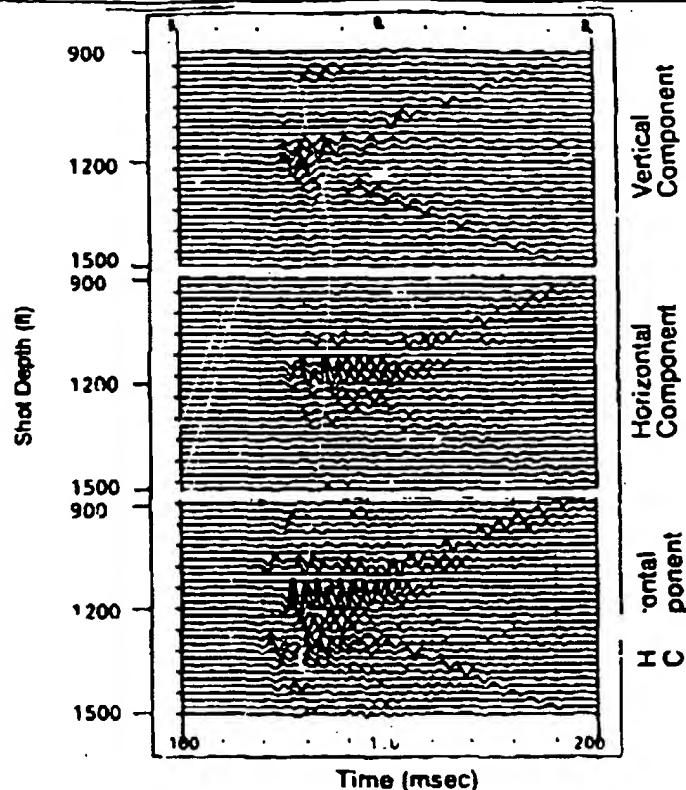


Figure 5. Common-receiver gather obtained from commercial VSP geophone sands. Sonde depth is 1200 ft, well-to-well spacing is 815 ft, and fixed display is used.

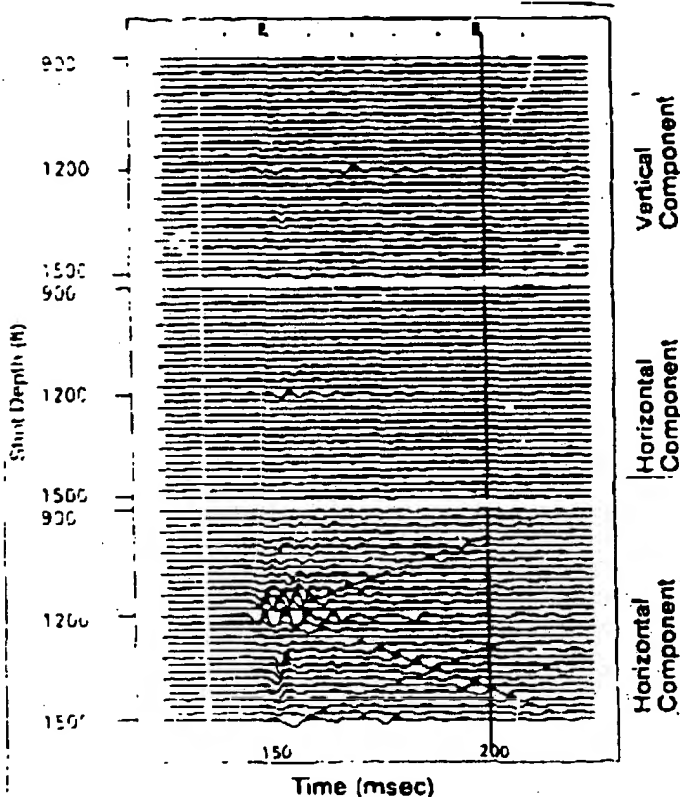


Figure 4. Common-receiver gather obtained from buried and cemented geophones. Geophone depth is 1187 ft, well-to-well spacing is 1215 ft, and fixed display gain is used.

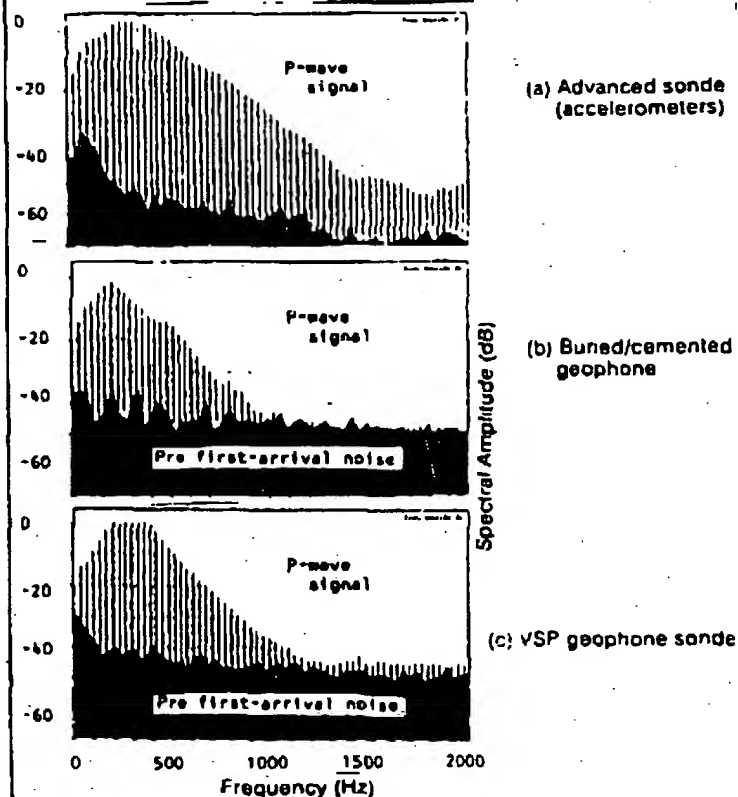


Figure 6. Spectral analysis of common receiver gathers. Both average horizontal-component p-wave spectra and pre-first-arrival noise spectra are shown.

NTIS does not permit return of items for credit or refund. A replacement will be provided if an error is made in filling your order, if the item was received in damaged condition, or if the item is defective.

Reproduced by NTIS

National Technical Information Service
Springfield, VA 22161

*This report was printed specifically for your order
from nearly 3 million titles available in our collection.*

For economy and efficiency, NTIS does not maintain stock of its vast collection of technical reports. Rather, most documents are printed for each order. Documents that are not in electronic format are reproduced from master archival copies and are the best possible reproductions available. If you have any questions concerning this document or any order you have placed with NTIS, please call our Customer Service Department at (703) 605-6050.

About NTIS

NTIS collects scientific, technical, engineering, and business related information — then organizes, maintains, and disseminates that information in a variety of formats — from microfiche to online services. The NTIS collection of nearly 3 million titles includes reports describing research conducted or sponsored by federal agencies and their contractors; statistical and business information; U.S. military publications; multimedia/training products; computer software and electronic databases developed by federal agencies; training tools; and technical reports prepared by research organizations worldwide. Approximately 100,000 *new* titles are added and indexed into the NTIS collection annually.

For more information about NTIS products and services, call NTIS at 1-800-553-NTIS (6847) or (703) 605-6000 and request the free *NTIS Products Catalog*, PR-827LPG, or visit the NTIS Web site <http://www.ntis.gov>.

NTIS

***Your indispensable resource for government-sponsored
information—U.S. and worldwide***

**This Page is Inserted by IFW Indexing and Scanning
Operations and is not part of the Official Record**

BEST AVAILABLE IMAGES

Defective images within this document are accurate representations of the original documents submitted by the applicant.

Defects in the images include but are not limited to the items checked:

- ☒ **BLACK BORDERS**
- ☒ **IMAGE CUT OFF AT TOP, BOTTOM OR SIDES**
- ☐ **FADED TEXT OR DRAWING**
- ☐ **BLURRED OR ILLEGIBLE TEXT OR DRAWING**
- ☒ **SKEWED/SLANTED IMAGES**
- ☒ **COLOR OR BLACK AND WHITE PHOTOGRAPHS**
- ☐ **GRAY SCALE DOCUMENTS**
- ☐ **LINES OR MARKS ON ORIGINAL DOCUMENT**
- ☐ **REFERENCE(S) OR EXHIBIT(S) SUBMITTED ARE POOR QUALITY**
- ☐ **OTHER:** _____

IMAGES ARE BEST AVAILABLE COPY.

As rescanning these documents will not correct the image problems checked, please do not report these problems to the IFW Image Problem Mailbox.